Late to post-Appalachian strain partitioning and extension in the Blue Ridge of Alabama and Georgia

Mark G. Steltenpohl[1], Joshua J. Schwartz[2], and B.V. Miller[3]
[1]*Department of Geology and Geography, Auburn University, Auburn, Alabama 36849, USA*
[2]*Department of Geological Sciences, California State University, Northridge, Northridge, California, 91330, USA*
[3]*Department of Geology & Geophysics, Texas A&M University, College Station, Texas 77843-3115, USA*

ABSTRACT

Structural observations and U-Pb and $^{40}Ar/^{39}Ar$ isotopic age dates are reported for shear zones and metamorphic rocks in the southernmost Appalachian Blue Ridge. Two major mylonite zones, the Goodwater-Enitachopco and Alexander City fault zones, have retrograded peak amphibolite facies fabrics and assemblages in rocks of the ancient Laurentian margin. Both faults are within a zone of transition between Carboniferous (Alleghanian) west-directed thrusts in the foreland and synchronous strike-parallel dextral shear zones in the hinterland. The $^{40}Ar/^{39}Ar$ hornblende and muscovite dates record late Mississippian cooling and exhumation from the Late Devonian (Neoacadian orogeny, 380–340 Ma) peak. Retrograde mylonites of the Goodwater-Enitachopco fault are of two types. Earlier formed, type 1, upper greenschist to lower amphibolite facies shears are roughly coplanar with the dominant schistosity of the country rock, and show northwest-southeast stretching. Later formed, type 2 shears are discrete, steeply dipping, middle to upper greenschist facies shear zones that cut across the type 1 shears, displacing them in an oblique dextral and normal slip sense. A 366.5 ± 3.5 Ma U-Pb SHRIMP-RG (sensitive high-resolution ion microprobe–reverse geometry) date on zircon from a prekinematic trondhjemite dike that is cut by a type 2 shear zone places a maximum age on the time of movement along the Goodwater-Enitachopco fault. The $^{40}Ar/^{39}Ar$ cooling dates place a minimum on the timing of extensional movement along the type 1 shears of between ca. 334 and 327 Ma. The Goodwater-Enitachopco fault coincides at depth with a basement step up that has been interpreted as a Cambrian rift fault formed along the ancient Laurentian margin, possibly reflecting its reactivation during Mesozoic rifting of Pangea.

The Alexander City fault zone is a middle greenschist facies, dextral strike-slip fault rather than a west-vergent thrust fault, as was previously thought. This fault zone is obliquely cut and extended by more east-trending, subvertical, cataclastic faults (Mesozoic?) characterized by intense quartz veining. These brittle faults resemble those in other parts of the Blue Ridge, Inner Piedmont, and Pine Mountain terrane and, together with the Goodwater-Enitachopco and Towaliga faults, they appear to form a broad graben-like structure across the entire piedmont. Shoulder rocks flanking the Alexander City fault zone contain earlier formed (peak to late peak metamorphic) dextral shear zones. A 369.4 ± 4.8 Ma U-Pb thermal ionization mass spectrometry date on zircon records the time of crystallization of a dike that cuts one of the shears bracketing the peak metamorphic fabric to between ca. 388 and 369 Ma and places a minimum age for right-slip shearing. Similar kinematics, geometries, tectonostratigraphic positions, and timing indicate that these Devonian shears are more southern counterparts to the system of Neoacadian dextral faults exposed in the North Carolina Blue Ridge.

Kinematic analysis of the Goodwater-Enitachopco and Alexander City faults document that dextral strains in the Alabama and western Georgia Blue Ridge are partitioned much farther toward the foreland than is reported to the northeast, likely as a consequence of the southern Appalachian master décollement having passed obliquely across a several kilometer step up along the Cartersville transform. The top-to-the-south-southeast normal-slip component of movement along the Goodwater-Enitachopco fault is unusual, considering its position far toward the foreland. Loose timing constraints for this extensional event (late Carboniferous to Early Jurassic) leave room for several tectonic explanations, but we favor the following. (1) Late Pennsylvanian to Early Permian crustal thickening created a wedge of Blue Ridge rocks bound above by the Goodwater-Enitachopco, below by the décollement, and to the northwest (present-day direction) by a topographically steep mountain front. (2) Further convergence and crustal thickening caused this wedge to gravitationally collapse with southward-driven motion. (3) Mesozoic rifting reactivated some of the faults as the Gulf of Mexico began to open.

INTRODUCTION

Following the paradigm shift to plate tectonic thinking in the mid-1960s, which explained how layer-parallel compressive stresses were derived from colliding continents, most southern Appalachian (eastern USA) mylonite zones were interpreted as west-directed thrusts. Thrust faults are classically documented in the southern Appalachian foreland fold and thrust belt (i.e., the Valley and Ridge physiographic province; Fig. 1), where fossiliferous Paleozoic sedimentary rocks indicate them to have formed during the late Carboniferous to Permian (the Alleghanian orogenic phase; Roeder et al., 1978; Woodward, 1957; Hatcher et al., 1989a). Development of methods to constrain the kinematics of fault zones based on shear-sense indicators in mylonitic rocks in the late 1970s and early 1980s (e.g., see references cited in Steltenpohl, 1988) led to the paradoxical discovery that practically all of the major Carboniferous to Permian mylonite zones within the exposed southern Appalachian hinterland record right-slip movement rather than thrusting (i.e., the Brevard, Towaliga,

Geosphere; June 2013; v. 9; no. 3; p. 647–666; doi:10.1130/GES00738.1; 13 figures; 3 tables; 1 supplemental file.
Received 25 July 2011 ♦ Revision received 31 January 2013 ♦ Accepted 19 February 2013 ♦ Published online 7 May 2013

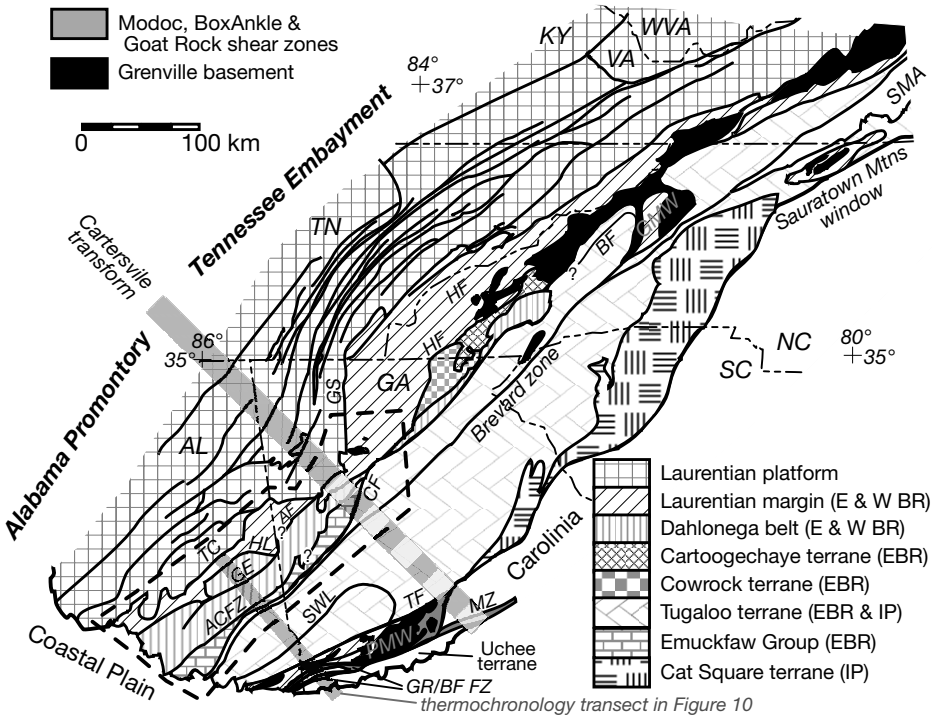

Figure 1. Tectonic map of the Southern Appalachians (modified from Hatcher et al., 1989b, 2007a; Hatcher, 2004; Hibbard et al., 2002, 2006; Steltenpohl, 2005; Steltenpohl et al., 2008). The Cartersville transform is dashed where we have extended it. Abbreviations: ACFZ—Alexander City fault zone; AF—Allatoona fault; BF—Burnsville fault; CF—Chattahoochee fault; E BR and W BR—Eastern and Western Blue Ridge; GE—Goodwater-Enitachopco fault; GMW—Grandfather Mountain window; GR/BF FZ—Goat Rock–Bartletts Ferry fault zone; GS—Great Smoky thrust; HL—Hollins Line fault; HF—Hayesville-Fries fault; IP—Inner Piedmont; MZ—Modoc zone; PMW—Pine Mountain window; SMA—Smith River allochthon; SWL—Stonewall Line shear zone; TC—Talladega-Cartersville fault; TF—Towaliga fault. Other letters in bold are state abbreviations.

Bartletts Ferry, Goat Rock, and Modoc fault zones depicted in Fig. 1; Secor et al., 1986; Steltenpohl, 1988, 2005; Hooper and Hatcher, 1988; Steltenpohl et al., 1992, 2010; Steltenpohl and Kunk, 1993; West et al., 1995). Such strain partitioning between the hinterland and foreland is also reported from the central and northern Appalachians, indicating that it is an orogen-wide phenomenon (e.g., Gates et al., 1988; Horton et al., 1989; Bothner and Hussey, 1999; Goldstein and Hepburn, 1999; Hatcher, 2002, 2010; Hatcher et al., 2007b). Today, how Alleghanian, orogen-parallel, dextral movement within the hinterland transitions to apparently synchronous across-strike thrusting in the foreland (Gates et al., 1988; Dallmeyer et al., 1986; Secor et al., 1986; Steltenpohl, 1988; Steltenpohl et al., 1992) remains an unresolved problem concerning the late Carboniferous to Permian tectonic evolution of the southern Appalachians. We lack a good explanation for how the orogen transitioned in the Permian from a thickened collisional welt into a collapsed and extending rift margin by the end of Triassic time (Sacks and Secor, 1990; Snoke and Frost, 1990; Steltenpohl et al., 1992; Maher et al., 1994; Carter et al., 2001).

To address the problem of how strain was partitioned between the Alleghanian foreland and hinterland, we examined fault rocks from two key mylonite zones in Alabama, the Goodwater-Enitachopco and Alexander City faults (Figs. 1 and 2). These two fault zones are within the eastern Blue Ridge, where the transition likely occurs. Both have been shown as northwest-directed thrust faults on some earlier maps (Higgins et al., 1988; Osborne et al., 1988), but no modern mesoscale or microscale kinematic and microstructural data have been reported. Here we report geometric, kinematic, and rheological analyses. Because the timing of movement along these fault zones is also largely unconstrained, we performed initial U-Pb zircon and $^{40}Ar/^{39}Ar$ muscovite and hornblende thermochronological analyses. Our results are surprising in that they indicate somewhat peculiar kinematic and timing histories that we believe hold important new insights into the late stages of tectonic evolution of the southernmost Appalachians.

GEOLOGIC SETTING

At the scale of a geologic map of eastern North America, stark differences in southern Appalachian structures are clearly seen between the Tennessee–western North and South Carolina–northern Georgia and the Alabama segments of the orogen (Fig. 1). Eastern Tennessee contains the classic, thin-skinned, southern Appalachian foreland fold-and-thrust belt with as many as 13 different, generally coplanar, northwest-directed thrusts. In sharp contrast, the Valley and Ridge of Alabama and western Georgia contains many fewer northwest-directed thrusts (see Fig. 1). The Cartersville transform corresponds to this transition and is interpreted to mark an ancient transform fault along the rifted Laurentian margin, separating the Tennessee embayment from the Alabama promontory (Fig. 1), which served as a template around which later-emplaced Appalachian sheets conformed (Thomas, 1991, 2006; Tull et al., 1998a, 1998b; Tull and Holm, 2005; Thomas and Steltenpohl, 2010). This thrust stack is directly west of the Great Smoky and Hayesville thrusts (Fig. 1) that have emplaced the western and eastern Blue Ridge terranes, respectively, upon the Laurentian platform (Fig. 1; Hatcher, 1987, 2010). The Talladega-Cartersville fault is the frontal Blue Ridge fault in Alabama and western Georgia and, like its structural equivalent the Great Smoky fault, is the southern Appalachian master décollement (Cook et al., 1979). The Talladega-Cartersville fault, however, is a complex structure containing major decapitated folds within klippen and fensters that do not follow conventional foreland fold-and-thrust-belt rules, such as those documented in Tennessee (Fig. 2; Tull, 1984; Tull and Holm, 2005).

The Hollins Line fault is the basal eastern Blue Ridge fault in Alabama and occupies a structural position equivalent to the Hayesville thrust (Bentley and Neathery, 1970; Hatcher, 1978; Tull, 1978, 1980, 1982, 1984, 1995; Steltenpohl and Moore, 1988; McClellan et al., 2005, 2007; Tull et al., 2007). Contrary to thrust movement along the Hayesville fault, the Hollins Line is an oblique, right-slip transpressional fault (Mies, 1991). Tull (1995) called it the "Hollins Line transpressional duplex: Eastern-Western Blue Ridge terrain boundary," and the duplex is large enough to be seen (in Fig. 2) directly west-southwest of the town of

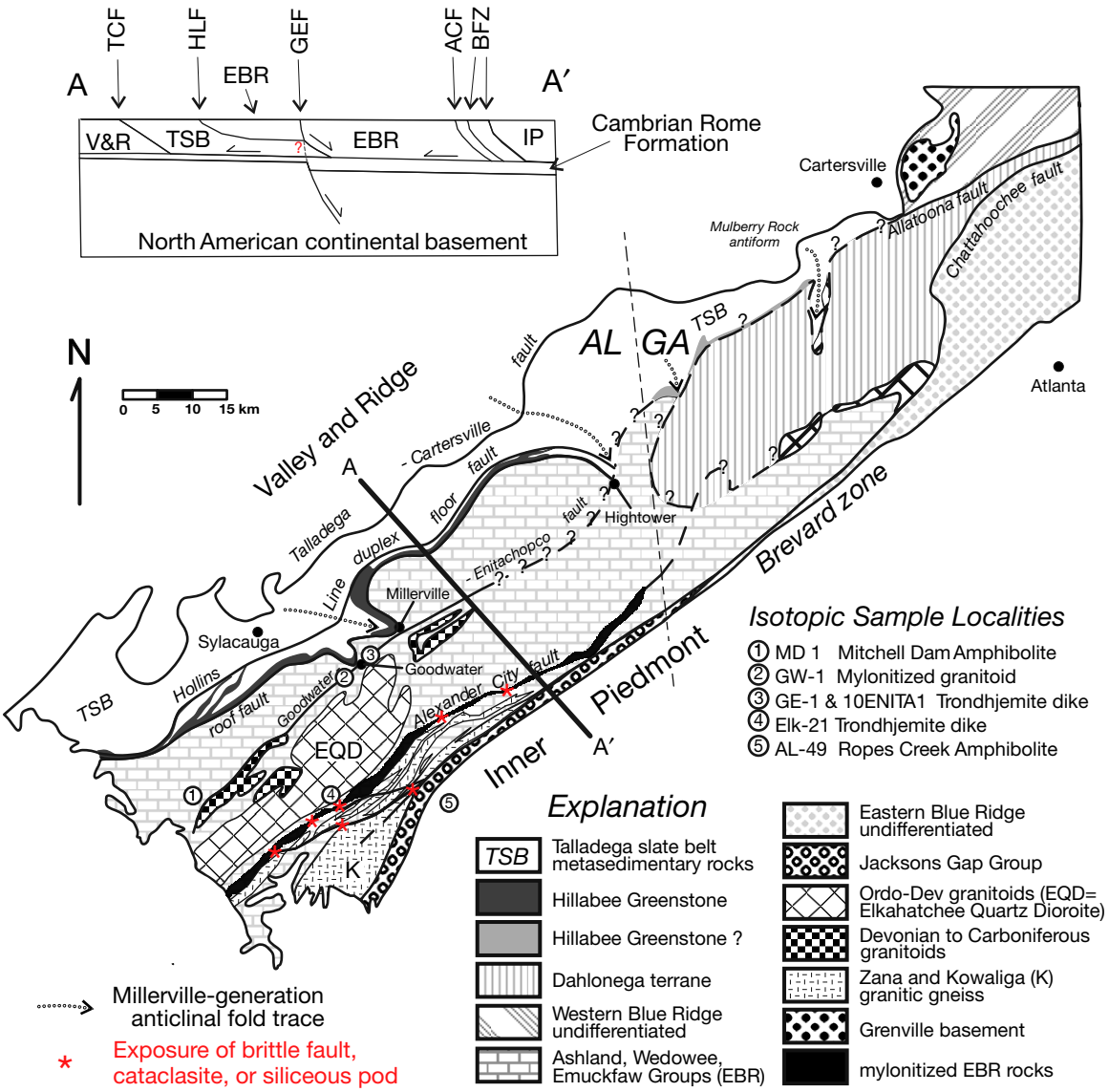

Figure 2. Tectonostratigraphic map of the Blue Ridge in Alabama (AL) and part of Georgia (GA) with major tectonic features described in this report (modified after Tull, 1984; McClellan et al., 2007). (Cross section is modified from Thomas et al., *in* Hatcher et al., 1989b; Thomas, 1991; Steltenpohl, 2005; Steltenpohl et al., 2008.) ACF—Alexander City fault; BFZ—Brevard fault zone; EBR—Eastern Blue Ridge; GEF—Goodwater-Enitachopco fault; HLF—Hollins Line fault; IP—Inner Piedmont; TFC—Talladega Cartersville fault; TSB—Talladega slate belt; V&R—Valley and Ridge; Ordo-Dev—Ordovician–Devonian.

Millerville. Right-slip movement in Alabama has therefore encroached farther toward the foreland than anywhere else within the orogen. Continuing southeastward, the Goodwater-Enitachopco and Alexander City fault zones are the next two Blue Ridge faults and the focus of our investigation. The Brevard fault zone marks the southeastern boundary of the eastern Blue Ridge, juxtaposing the Inner Piedmont terrane (Figs. 1 and 2), and is a polyphase, right-slip shear zone with both Neoacadian (ca. 380–340 Ma) and Alleghanian movement histories (Bobyarchick, 1983, 1999; Vauchez, 1987; Bobyarchick et al., 1988).

Additional background information on the lithologies, structures, metamorphism, and plutonic igneous history of rocks in the Alabama and western Georgia Blue Ridge are provided in the Supplemental File[1].

[1]Supplemental File. PDF file of background materials. If you are viewing the PDF of this paper or reading it offline, please visit http://dx.doi.org/10.1130/GES00738.S1 or the full-text article on www.gsapubs.org to view the Supplemental File.

STRUCTURAL AND KINEMATIC ANALYSES

Goodwater-Enitachopco Fault Zone

Our mapping of mylonites and phyllonites associated with the Goodwater-Enitachopco fault does not indicate a simple single-strand fault, as shown on earlier maps. Rather, two types of shears, referred to as type 1 and type 2 shears, generally occur along the trace of the fault depicted in Figure 2. Type 1 shears formed

at higher temperatures and are roughly coplanar with the dominant schistosity (S_1) of the middle to upper amphibolite facies country rock. Later-formed, type 2 shear zones are discrete, steeply dipping, and tabular, and they cut cleanly across S_1 and the type 1 shears. Both types of shears can be difficult to recognize given the scarcity and poor quality of exposures (saprolite), but the high-angle offsets and steep dips of the later-formed shear zones make them easier to recognize in the field.

Type 1 shears do not appear to form a single, tabular shear zone, but rather occur randomly at various structural levels generally northeast of Millerville, Alabama (Fig. 2). Mylonitic fabrics in schist, granite, and pegmatite are roughly coplanar with the S_1 schistosity (Fig. 3A), and the quartz and K-feldspar elongation lineations are predominantly downdip, plunging moderately to shallowly to the south-southeast (Fig. 4A). Type 1 shear zones commonly are cut at a high angle by steeper dipping type 2 shear zones (Fig. 3B). Shear-sense indicators in type 1 mylonitized pegmatite can be ambiguous where the feldspar porphyroclasts interfere with one another, and there is also a fairly high degree of orthorhombic symmetry (Fig. 3C), but the downdip elongation direction (Fig. 4A) documents south-southeast–north-northwest stretching. In more strongly comminuted rocks (e.g., bottom of the slab in Fig. 3C), however, ribbon structures, sigma clasts, microfolds, and S-C fabrics (Figs. 3A and 4A) record top-down-to-the-south-southeast normal-slip movement. Large feldspar porphyroclasts (to 4.5 cm in diameter) have distinct core-mantle structures observable at the hand-specimen scale (Fig. 3C); cores are cracked, whereas rims have a 1–2-mm-thick sheath of finely recrystallized feldspar. Otherwise, feldspar occurs as smaller augen that range down to finely recrystallized grains within several-millimeter-thick ribbons. Overall, feldspar microstructures indicate upper greenschist to lower amphibolite facies conditions of mylonitization (450–600 °C; Passchier and Trouw, 1996). These conditions are consistent with type 1 mylonites found in other host lithologies where synkinematic hornblende and biotite recrystallized via grain-boundary migration recrystallization (Regime 3 of Hirth and Tullis, 1992), and rolled garnet porphyroblasts reflect near metamorphic peak deformational conditions. The type 1 buttony fabric in pelitic lithologies generally occurs without much microstructural evidence of nonrecovered strain, implying that shearing likely began far beneath the ductile-brittle transition (Sibson, 1977) during the waning stages of metamorphism following the peak.

Type 2 shear zones (Fig. 5) appear to be mostly developed in the segment of the Goodwater-Enitachopco fault where it interacts with the Millerville anticline (i.e., reentrant; Fig. 2). These late shears range in thickness from <1 m to nearly 5 m, and they appear to be randomly spaced though generally <100 m apart from one another. Lower hemisphere stereographic projections of type 2 shears (Fig. 4A) indicate a range of strike orientations, from N17°E to N88°E, and dips averaging ~67°SE. Compositional layering, the S_1 foliation, and tabular (<0.5 m thick) sill-like granitic injections are drag folded where crosscut by the type 2 shears, consistently indicating oblique-normal and/or right slip, top-down-to-the-south movement (Fig. 5A). Type 2 shear zones typically are marked by phyllonites, or button schists, with well-developed S-C fabrics that clearly record oblique dextral and normal sense of shear (Figs. 5B, 5C). Composite S-C planar fabrics were

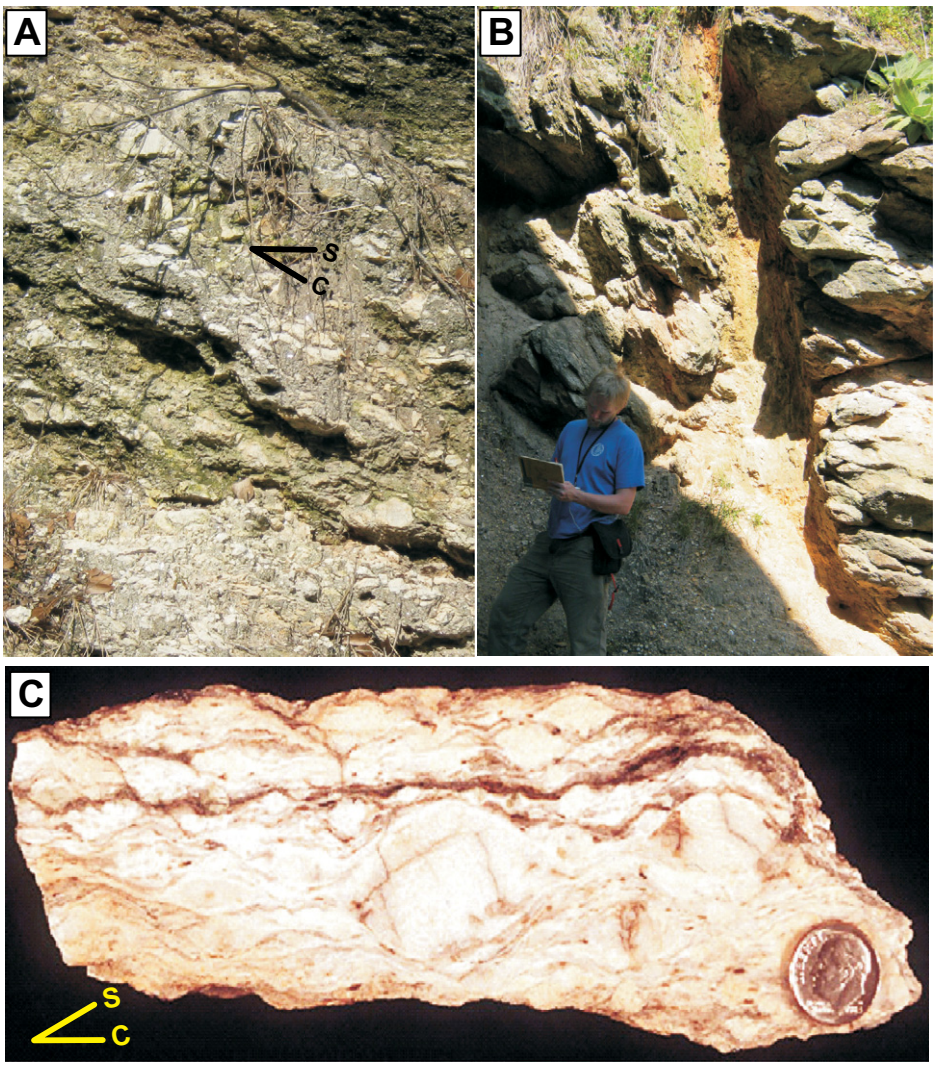

Figure 3. Type 1 shears of the Goodwater-Enitachopco fault. (A) Mylonite fabric in pegmatite and encapsulating muscovite-quartz schist. C-planes are tilted shallowly to the right whereas S-planes are subhorizontal, indicating downdip normal-slip movement. Height of view is ~1 m. (B) Steeply east dipping (toward right in photo) type 2 shear zone that cuts a 3-m-thick type 1 shear zone within a pegmatite body. Mylonitic foliation dips shallowly to the east but is steepened due to normal-slip drag on the west margin of the type 2 fault. (C) Polished slab of the type 1 mylonitized pegmatite sample GW-1 collected from the outcrop shown in B (33°03′57.78″N, 86°03′12.21″W); muscovite was separated from this sample for $^{40}Ar/^{39}Ar$ dating. Sample is oriented parallel to the downdip elongation lineation and perpendicular to the mylonitic foliation. Strain geometry reflects a moderate orthorhombic component, but top-down-to-the-southeast normal-slip movement is indicated by C′ surfaces and sigma clasts.

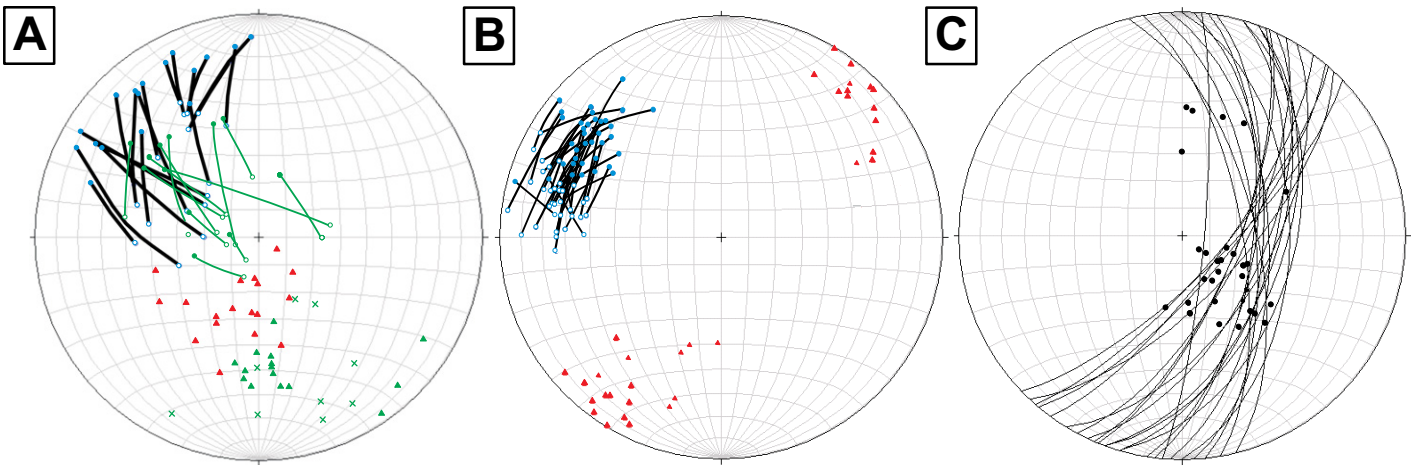

Figure 4. Lower hemisphere equal-area stereoplots; north is at the top of each diagram. (A) Poles to S (blue circles; n = 18) and C (blue dots; n = 18) planes and slip lines (red triangles; n = 18) from type 2 shear zones of the Goodwater-Enitachopco fault. Black arcs connect S-C pairs, slip lines were geometrically determined (see text); green symbols are for type 1 shear zones ($n_s = n_c = n_{sliplines} = 11$). X symbols are measured elongation lineations (n = 9). (B) Same elements described in A, but for the Alexander City fault zone ($n_s = n_c = n_{sliplines} = 36$). (C) Reverse-slip crenulations (RSCs) measured in the Alexander-City fault zone. Black dots are crenulation fold hinges (n = 31) and great circles are RSCs (n = 24).

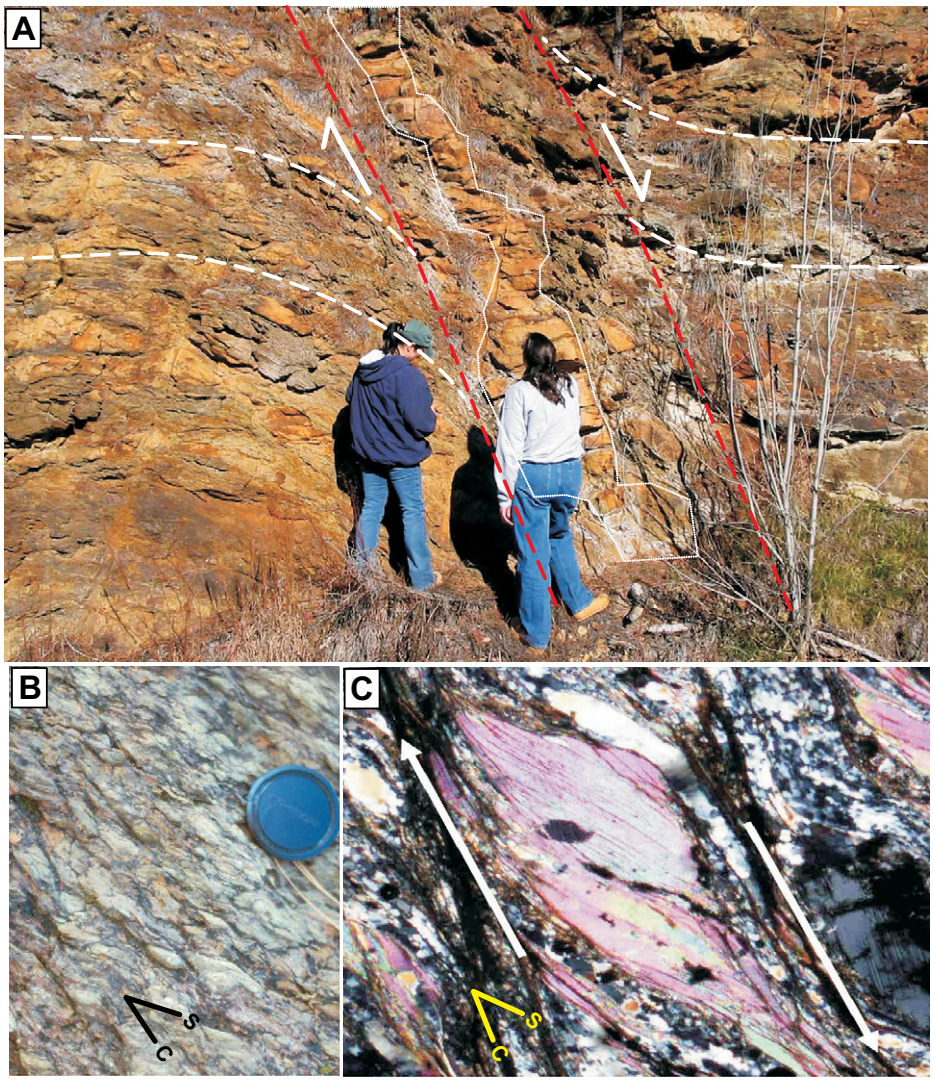

Figure 5. Type 2 shear zone of the Goodwater-Enitachopco fault (33°02′09.33″N, 86°07′18.43″W). (A) Mesoscopic drag folds in schistosity, compositional layering, and a trondhjemitic dike along the steeply southeast dipping (right in photo) shear zone clearly indicate normal-slip separation. Subhorizontal fractures in the dike reflect the weak mica foliation. U-Pb isotopic sample 10ENITA1 was sampled from this dike. (B) Closeup view of a vertical outcrop face showing S-C fabrics looking parallel to the shallow-northeast-plunging intersection between the composite fabrics. Here sense of shear is predominantly normal slip with a minor right-slip oblique component. (C) Photomicrograph, in cross-polarized light, of mica fish, S-C fabrics, and quartz tails, from an oriented sample of the phyllonite shown in B.

measured and geometrically examined using lower hemisphere, equal-area stereoplots of paired C- and S-planes (connected by great circle arcs in Fig. 4A). Slip lines were constrained as being within the C-plane 90° from their intersection with the S-plane. Slip lines plunge 55° downdip with a slight southwest trend, implying that slip was mostly normal top down to the south. Figure 4A indicates that more eastward-trending faults have a stronger tendency toward right-lateral strike-slip components, whereas more northward faults, which appear concentrated near the Millerville reentrant, have more downdip normal-slip components.

Microscopic analysis of phyllonites from type 2 shear zones reveals asymmetric mica fish and muscovite-quartz composites that consistently verify oblique right-lateral and normal-slip movement (Fig. 5C). Quartz microstructures are mostly subgrains and minor amounts of grain-boundary bulges, reflecting the operation of subgrain rotation recrystallization and grain-boundary migration during dynamic recrystallization (Regime 2 and 3 microstructures of Hirth and Tullis, 1992). Feldspar microstructures include grain-boundary bulges along rims, weak core-mantle structures, and broad microkinks in grain cores. Quartz and feldspar microstructures indicate medium-range temperature conditions for mylonitization between ~450 and 600 °C (Tullis, 1983, 2002; Simpson and Schmid, 1983; Scholz, 1988; Tullis and Yund, 1992; Hirth and Tullis, 1994; Passchier and Trouw, 1996), probably near the lower end of this temperature range. Inferred deformational temperatures for the type 2 mylonites therefore indicate that they formed beneath the ductile-brittle transition.

Steeply southeast dipping, tabular, weakly foliated trondhjemite injections are commonly found within the type 2 Goodwater-Enitachopco shears (Figs. 5 and 6). Compositionally similar trondhjemites occur as boudinaged layers outside of the type 2 shears, where they roughly parallel the shallow-dipping compositional layering and/or metamorphic foliation, S_1, within the country rock. Where these prekinematic sill-like injections are cut by type 2 shears, they are dragged and folded into the shear zone with phyllonites developed generally <1 m into the bounding host schists (Fig. 5A). Strain internal to these intrusions is accommodated along discrete, thin (several millimeters thick), domino- or bookshelf-style normal faults (Figs. 6E, 6F). While most of the trondhjemites are sill-like injections, other generally thicker (to 1 m) and more tabular dike-like bodies intruded at a high angle to the compositional layering and metamorphic foliation of the host rock. Type 2 shear zones are best developed along these dike-like trondhjemite bodies, indicating that they were favorably oriented for high resolved shear stress during oblique dextral-normal movements. Metamorphic foliation is only feebly developed within the dike-like and sill-like injections, implying that they were intruded either during the waning stages of Neoacadian metamorphism or perhaps during early Alleghanian strains. Fluids associated with shearing have altered some of the prekinematic injections. Country-rock margins to altered dikes are commonly marked by a parallel quartz vein (Fig. 6A), some as thick as ~30 cm. The altered dikes have diffuse zonations that reflect a pristine, medium gray, biotite-muscovite metatrondhjemite core, an intermediate zone of green, epidotized trondhjemite, and a light gray, mica-poor and quartz-rich metatrondhjemite at the dike rim (Fig. 6A). Microscopically, quartz porphyroclasts (>0.5 mm) typically have strong patchy and undulose extinction with smaller elongate subgrains (0.2–0.5 mm) (Fig. 6C), whereas in quartz-rich regions near the dike margins quartz has more lobate and sutured grain boundaries (Fig. 6B). The combination of subgrains and lobate grain boundaries suggests that subgrain-rotation recrystallization and grain-boundary migration were active recovery processes during fluid-assisted shearing. Plagioclase feldspar cores exhibit alteration to fine-grained white mica. Secondary clinozoisite and epidote are also associated with fine-grained white mica (Fig. 6C).

Some type 2 shear zones appear to have been intruded by synkinematic trondhjemite injections. Synkinematic injections may occur as multiple veins within the same shear zone and the phyllonitic fabrics marginal to them display a similarly oriented, steeply dipping planar fabric. Internally, the synkinematic trondhjemite dikes display a weak subvertical foliation defined by planar alignment of muscovite, biotite, and plagioclase (Fig. 6D). Dike cores are medium grained and contain aligned plagioclase phenocrysts to 0.5 cm in length, and grain size progressively decreases toward the dike margins over an ~5-cm-thick interval. Xenoliths of schist within the trondhjemite contain S-C shear fabrics that are coplanar with and look identical to those observed in the adjacent country rock (Fig. 6D), supporting synkinematic injection. Synkinematic trondhjemites contain no obvious petrographic evidence for sillimanite-grade mineral assemblages or fabrics related to the peak metamorphic event that affected the adjacent Higgins Ferry Group country rock.

Alexander City Fault Zone

Retrograde mylonites of the Alexander City fault zone are observed within rocks of the Wedowee and Emuckfaw Groups, as well as the Paleozoic granitic bodies that have intruded them (Fig. 2). The main ductile shear zone is within Wedowee metapelitic rocks, which served to localize strain due to their lower competence as compared to the shoulder rocks that are predominately granitic batholiths (i.e., Elkahatchee Quartz Diorite and Kowaliga Gneiss; Fig. 2). The shear zone thins and thickens drastically along strike from less than a few meters to as much as ~75 m (Fig. 2).

Mylonites and phyllonites of the Alexander City fault zone that are derived from the comminution of metasedimentary protoliths are marked by a stark color contrast between the alternating, centimeter-scale (and finer), dark and light bands (biotite- and quartz-rich layers, respectively) that clearly display the sense of shear within the zone (Figs. 7A, 7B). Sigma clasts of feldspar, mesoscopic and microscopic asymmetric folds (Fig. 7A), normal-slip crenulations (Fig. 7B), reverse-slip crenulations (Dennis and Secor, 1987), and well-developed S-C fabrics, consistently record right-slip movement. Microscopic kinematic and structural analysis of oriented samples substantiates the dextral shear sense observed in the field. Mica fish (Fig. 7C) and crystal-plastic deformation of quartz via grain-boundary migration recrystallization (Fig. 7D; Regime 1 of Hirth and Tullis, 1992) indicate middle greenschist facies, sub–ductile-brittle transition conditions for mylonitization. Quartz ribbons (Figs. 7B, 7D; Passchier and Trouw, 1996) are deformed into microfolds, further corroborating dextral rotational strain (Figs. 7A, 7C). Euhedral garnet porphyroclasts have strain shadows and are wrapped by asymmetric micas, suggesting prekinematic garnet growth and later rotation of the competent garnet grains. Both brittle fracturing of larger feldspar cores and grain-boundary bulging and recrystallization along the rims are observed in some larger porphyroclasts.

Lower hemisphere, equal-area stereographic analysis of measured C- and S-planes (Fig. 4B) further document predominantly right-slip movement recorded in mylonites and phyllonites. An oblique normal-slip (more downdip) component recognized in some outcrops is also indicated in Figure 4B. C- and S-plane point maxima are oriented N44°E, 64°SE and N16°E, 64°SE, respectively. Slip lines were stereographically determined with maxima at N46°E, 4° and S31°W, 22°, documenting mainly strike parallel movement. Minor oblique normal- and reverse-slip components in Figure 4B partly result from two sets of crenulations developed due to acute clockwise (normal-slip crenulations) and counterclockwise (reverse-slip crenulations) inclinations with respect to the shear zone movement direction. Reverse-

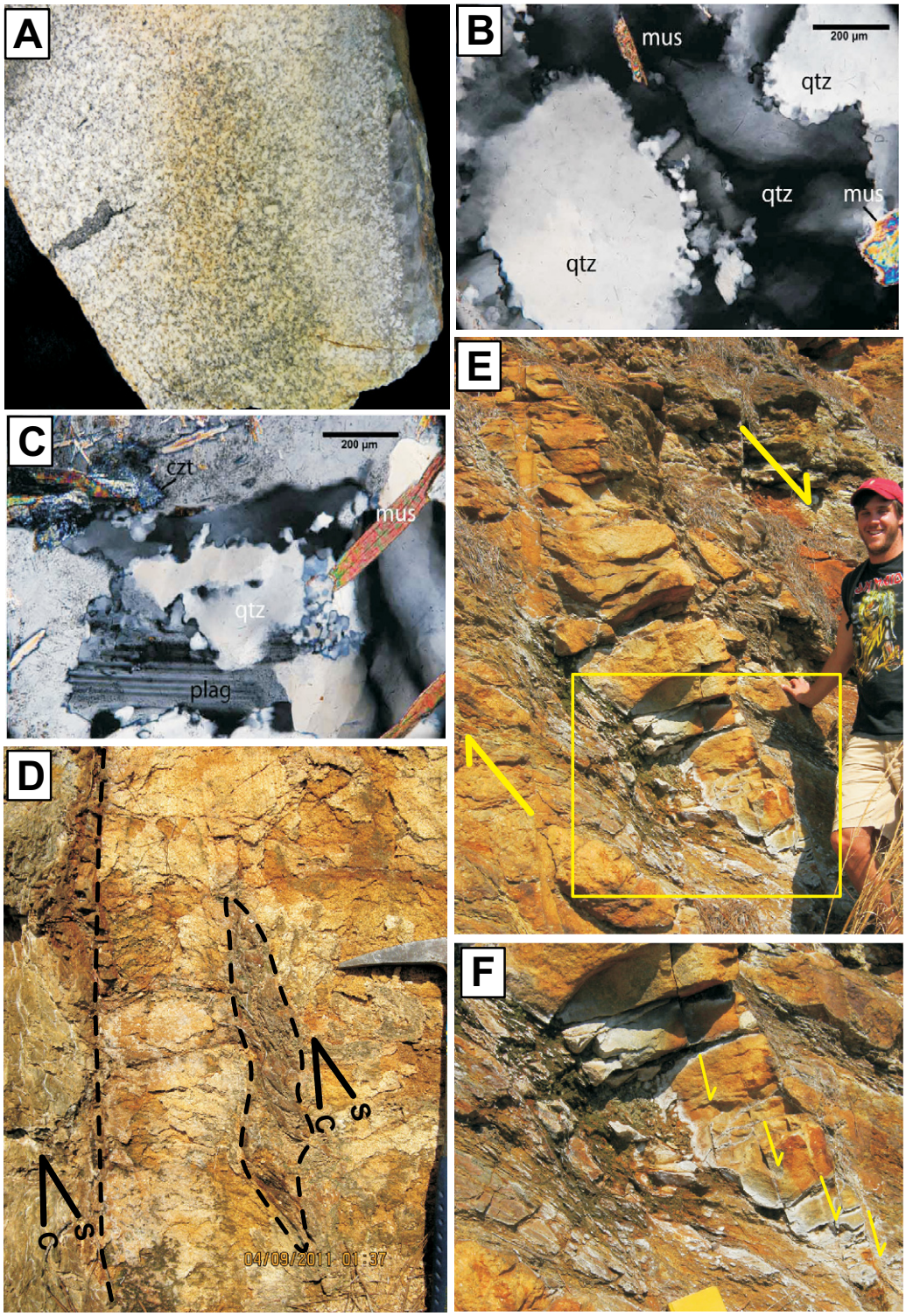

Figure 6. Field and petrographic images of trondhjemite bodies within type 2 Goodwater-Enitachopco shears. (A) Polished slab of prekinematic trondhjemite dike sample GE-1 used for $^{40}Ar/^{39}Ar$ dating of muscovite; sample was collected from the dike pictured in Figure 5A. Slab view is 14 cm in height. Slab is oriented as in the outcrop looking northeastward, with the weak mica foliation (tilted slightly left) paralleling the black flattened xenolith (left center), and a quartz vein (right) marking the southeast margin of the dike. Grain size fines toward the dike margin. Mineralogical zonation (left to right) reflects pristine biotite-muscovite metatrondhjemite in the core (white), epidotized zone (greenish, center), and mica-poor metatrondhjemite at the dike margin (light gray). (B) Photomicrograph of GE-1 (crossed polars). Subgrain development and lobate grain boundaries in quartz (qtz; mus—muscovite). (C) Photomicrograph of GE-1 (crossed polars). Lobate grain boundaries in quartz, large primary muscovite forms the foliation, and clinozoisite (czt) and fine-grained epidote (not pictured here) are common secondary alteration minerals (plag—plagioclase). (D) Xenolith or apophysis (outlined with dashed polygon) of normal-slip phyllonite incorporated into a synkinematic dike. Sense of shear in the included phyllonite is identical to that in the shear zone along the dike margin (vertical dashed line). (E) Type 2 normal-slip shear zone cutting subparallel to a prekinematic trondhjemite dike. Outlined area is F. (F) Bookshelf normal faults (steeply dipping to the right) have further extended the dike.

slip crenulations (Fig. 7A) were measured and examined by plotting the planes and hinge axes (Fig. 4C). Generally, S-C planes are roughly coplanar with reverse-slip crenulation planes, and the axes are spread along a partial great circle with a maximum being downdip (Fig. 4C). The boundaries of the Alexander City fault appear to roughly parallel the southeast-dipping mylonitic foliation. Trains of distinct phacoidal-shaped biotite-rich layers (~1 cm thick) observed in outcrops are extended along more east-trending normal-slip crenulation planes (e.g., Fig. 7B). These normal-slip crenulations appear to mimic the overall map pattern of the Alexander City fault zone shown in Figure 2, and several of them can be traced for tens of kilometers eastward to merge with the Brevard fault zone.

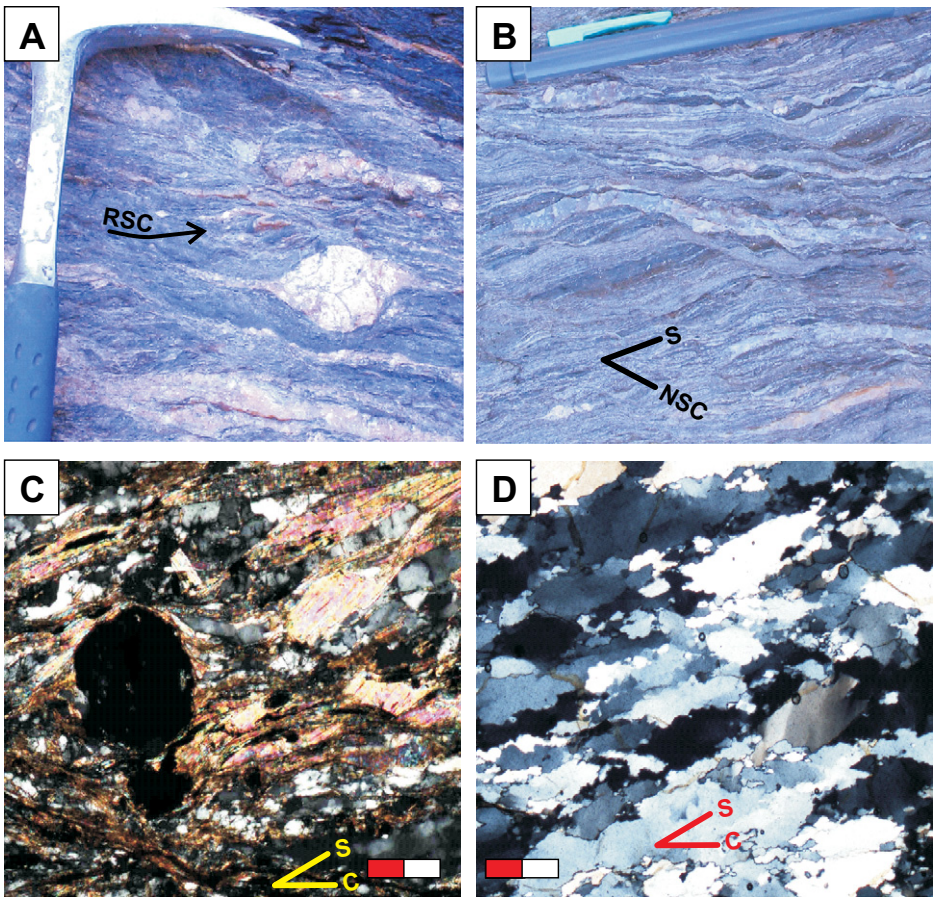

Figure 7. Field photos and photomicrographs of rocks within the Alexander City fault zone, all documenting right-slip displacement. (A) Outcrop photo of a quartz sigma clast and reverse-slip crenulations. Hammer head/pick is 18 cm long. (B) Field photo of normal-slip crenulations (NSCs). (C) Photomicrograph (plane-polarized light) of strain-shadow micas around a garnet and mica fish. Scale bar is 200 µm. (D) Photomicrograph (plane-polarized light) of quartz subgrain boundaries with prominent stepping up to the right. Scale bar is 200 µm.

The Alexander City fault zone is obliquely cut and extended by several subparallel to N60°–75°E striking, subvertical, brittle faults characterized by intense fracturing and veining, breccias, cataclasite, and silicified pods of cataclasite (Figs. 2 and 8). Several of these brittle faults locally correspond with and cut the ductile normal-slip crenulation splays that trend toward the Brevard zone (Fig. 2). These supra–ductile-brittle transition faults are marked by silicified breccia zones ("flinty crush rock") as much as 10 m thick that form narrow erosionally resistant ridges that have been quarried on a small scale for road metal (Fig. 8A). In outcrops, crosscutting quartz veins indicate polyphase fracturing events with the latest veins lacking evidence for attrition. In thin sections, the cataclasites contain evidence of multiple phases of brecciation and veining (Fig. 8B). The latest-formed quartz veins tend to be more tabular and continuous and are the coarsest grained (to 500 µm) with curved, well-equilibrated triple-point grain boundaries. The matrix is mostly fine-grained to very fine grained fragmented and granulated quartz and minor feldspar. Under ordinary light, dark gray to black clasts of more finely brecciated, commonly foliated, ultracataclasite occur in the matrix. Clasts of ultracataclasite contain internal veins of quartz, and the clasts are also cut by quartz veins (Fig. 8B). Associated with some of the brittle faults are infrequent but rather large cataclastic pods (<3 m thick and 7 m long) comprising breccias and cataclasites and large volumes of coarse-grained (to 3 cm in length) injected bull quartz (Fig. 8C). Samples from these pods resemble those from thicker (to 15 cm thick) quartz veins found elsewhere in the supra-ductile-brittle transition faults. These rocks are characterized by very large (to 3 cm long) quartz crystals that commonly have pyramidal terminations, rarely with double terminations, that give the rock a dog-tooth appearance. In thin sections (Fig. 8C), these quartz crystals contain multiple optical growth zones marked by varying concentrations of mineral and/or fluid inclusions, and the zones commonly have differing densities and orientations of fractures occurring in roughly subparallel sets. In addition to the fractures, microstructures include undulose extinction and subgrains, and minor volumes of very fine grained crystallized quartz filling interstitial spaces between the larger prisms. Sense of shear is difficult to determine in the cataclasites, but slickensides with slickenlines plunging moderately to steeply S68°W imply that the latest movement was oblique normal slip and right slip.

Dextral Shears in Alexander City Fault Zone Shoulder Rocks

While mapping shoulder rocks that flank the Alexander City fault zone we discovered high-temperature, peak to late peak metamorphic mylonitic shears that roughly parallel the zone and indicate the same right slip sense of shear (Fig. 9). They are notably persistent and particularly well developed in plutonic rocks on both sides of the fault zone (Fig. 9). We did not examine these mylonites in detail, and additional mapping and structural analysis will be needed to understand their significance. One exceptional area, however, was examined where the dextral shears are exposed in pavement of the Paleozoic (ca. 388–370 Ma) Elkahatchee Quartz Diorite (see sample locality 4 in Fig. 2, and Figs. 9A, 9B). The Elkahatchee Quartz Diorite has been metamorphosed to sillimanite-zone conditions and here the metamorphic foliation strikes N33°E and dips steeply toward the southeast. Steeply southeast dipping, N67°E striking, right-lateral strike-slip shear zones cut xenoliths and pegmatitic veins within the Elkahatchee (Fig. 9A). Dextral sense of rotation along these noncoaxial simple shear zones is recorded by trains of sigma clasts, normal-slip crenulations, and locally well-developed S-C composite planar fabrics (Fig. 9B). Quartz and feldspar are crystal-plastically deformed, indicating temperatures of deformation in excess of ~450 °C and up to peak metamorphic conditions. Figure 9B documents that along the immediate shoulders of the sheared pegmatite, the quartz diorite is mylonitized over an ~5 cm interval before the mylonitic foliation disappears, blending with the metamorphic foliation. At this locality, a late-stage trondhjemite dike cuts across the dextral shear zones (Fig. 9A), providing an opportunity to date the dike and to place constraints on the timing of this newly recognized dextral shearing event (see following).

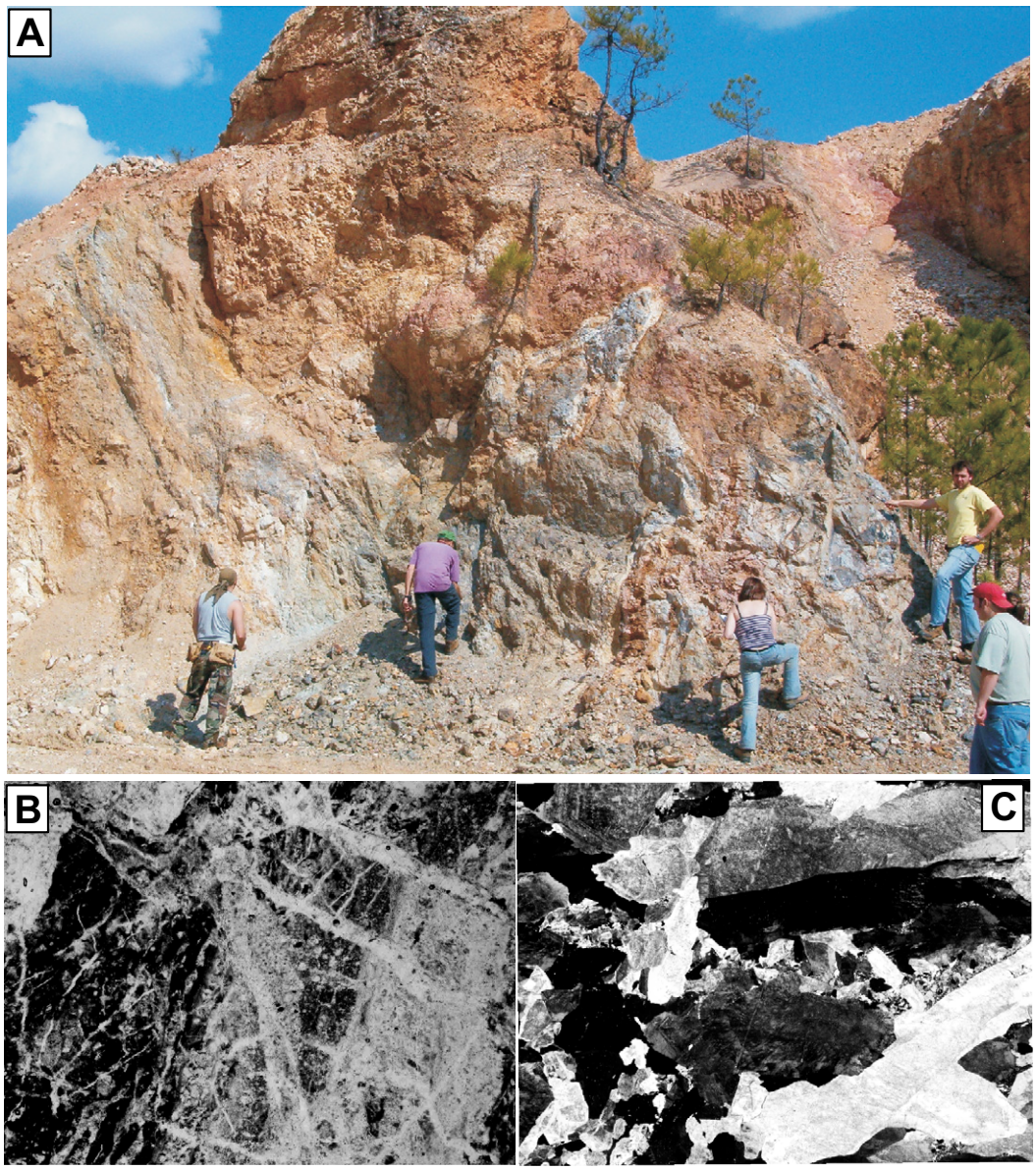

Figure 8. Field photos and photomicrographs of cataclastic rocks associated with the Alexander City fault zone. (A) Abandoned quarry (borrow pit) highwall providing a cross section through a cataclastic siliceous pod within the Alexander City fault zone. Gray areas, such as the one on the right being pointed at by the person in the yellow shirt, are highly indurated, intensely silicified and veined rock, which supports this linear ridge. (B) Photomicrograph (crossed polarized light) of brecciated mylonite from the quarry in A. Dark ultramylonite clast has mylonitic foliation tilted steeply to the left in the photomicrograph. Cloudy quartz veins have varying sized clasts and mineral and fluid inclusions, and are cut by later, clear nonattritional (implosion type) quartz veins. Long dimension of the field of view is 2500 μm. (C) Photomicrograph (plane-polarized light) of siliceous cataclastic rock. Injected bull quartz is characterized by euhedral quartz crystals with pyramidal terminations and multiple optical growth zones marked by varying concentrations of mineral and/or fluid inclusions. Fine-grained material filling interstices is both matrix-clast material and recrystallized quartz. Long dimension of the field of view is 5000 μm.

$^{40}Ar/^{39}Ar$ AND U-Pb ISOTOPIC DATING

The timing of movement along the Goodwater-Enitachopco, Alexander City, and newly discovered dextral Elkahatchee shear zones is critical to understanding the tectonic history of the southernmost Appalachian Blue Ridge. We present results from high-precision hornblende and muscovite $^{40}Ar/^{39}Ar$ and zircon U-Pb isotopic age-dating analyses. The $^{40}Ar/^{39}Ar$ dates (samples MD-1, GW-1, GE-1, and AL-49) constrain the time of mineral cooling through particular blocking temperatures (see McDougall and Harrison, 1999). The $^{40}Ar/^{39}Ar$ analyses were performed at the U.S. Geological Survey laboratory (Denver, Colorado) following the methods reported in Steltenpohl and Kunk (1993). U-Pb zircon analyses for sample Elk-21 were performed using facilities at the University of North Carolina and the analytical methods followed are the same as those described in Ratajeski et al. (2001). U-Pb zircon analyses for sample 10ENITA1 were performed using facilities at the Stanford–U.S. Geological Survey SHRIMP-RG (sensitive high-resolution ion microprobe–reverse geometry) facility following methods in Schwartz et al. (2011b). Sample localities are provided in Figure 2 and in Table 1.

$^{40}Ar/^{39}Ar$ Analyses and Their Interpretation

Hornblende sample MD-l is from the Mitchell Dam Amphibolite (Figs. 2 and 10). The hornblende grains constitute part of the peak metamorphic assemblage, together with plagioclase, quartz, titanite, and opaque minerals, in this middle amphibolite facies rock. The plateau age of 333.8 ± 1.7 Ma is somewhat younger than the Ordovician–Late Devonian range of conventional K-Ar dates for the same rock unit previously reported by Wampler et al. (1970; 348 Ma) and Russell (1978; 464–365 Ma); conventional K-Ar dates are known to give anomalously old apparent age dates, particularly in metamorphic rocks, because older extraneous gas components are not discernible using that technique (McDougall and Harrison, 1999). The 333.8 ± 1.7 Ma date is interpreted as the time of cooling through closure (~500 °C for hornblende), indicating that the rock maintained amphibolite facies temperatures well into the late Mississippian.

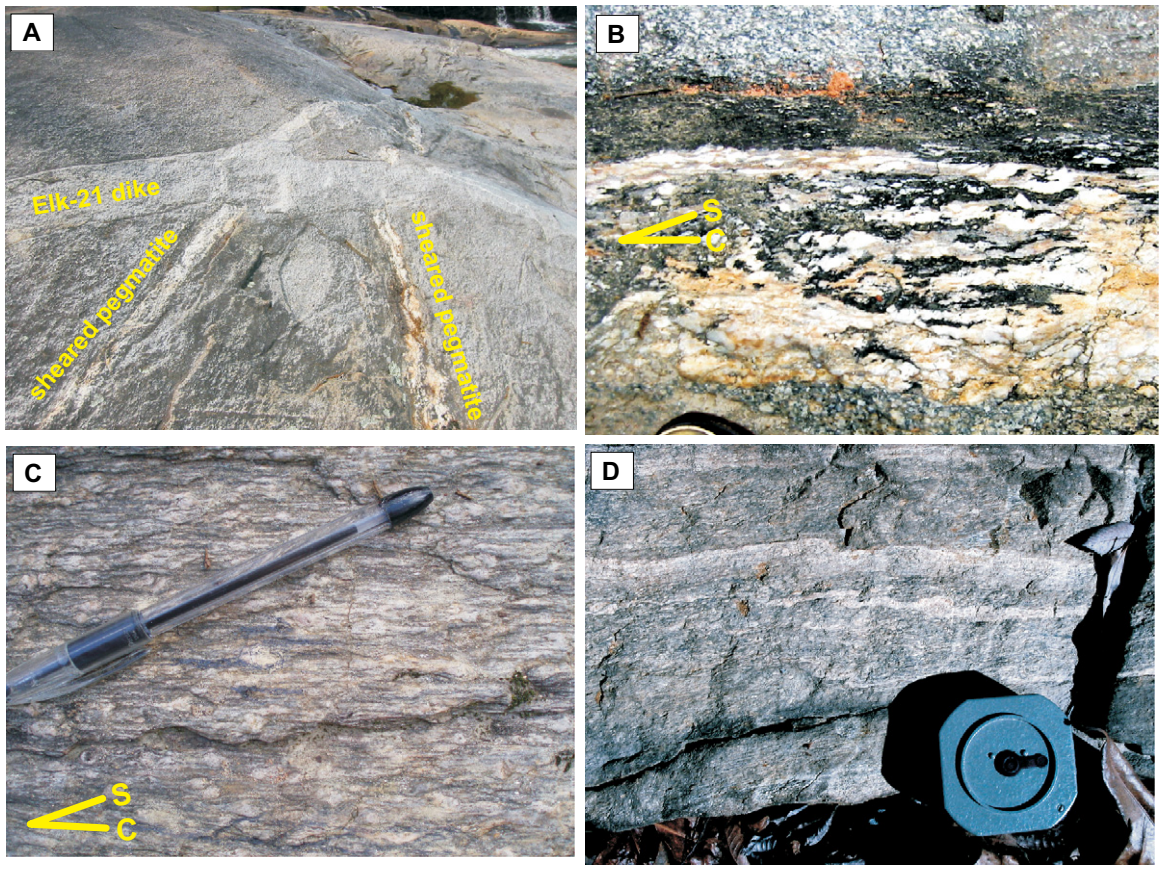

Figure 9. Mylonites and related features in adjacent shoulder rocks of the Alexander City fault zone. (A) Elkahatchee Quartz Diorite locality (32°54′05.36″N, 85°59′40.85″W). Trondhjemite dike (lighter gray, trending right to left center) from which sample Elk-21 was collected, cutting sheared pegmatitic veins. Dike is ~0.75 m thick (keys, just above center, provide scale). (B) Closeup view of sheared pegmatite in A displaying right-slip S-C fabrics and sigma-type porphyroclasts. Note progressive mylonitization of the Elkahatchee Quartz Diorite (darker gray at top of photo) over an ~5 cm interval along the upper margin of the pegmatite. Long dimension of the photograph is ~30 cm. (C) Typical dextral S-C mylonite in Zana Granite along the southeast shoulder. (D) Dextral folds of ultramylonite bands in granite along the northwest shoulder.

Hornblende grains separated from a massive amphibolite within the Ropes Creek Amphibolite of the Dadeville Complex (Bentley and Neathery, 1970; Steltenpohl et al., 1990a, 1900b) in the Inner Piedmont (Figs. 2 and 10), sample AL-49, were also analyzed for $^{40}Ar/^{39}Ar$ isotopes. The hornblende grains form a moderately well developed nematoblastic fabric recording peak amphibolite facies metamorphic conditions. The spectrum is only slightly discordant with a weak saddle shape that has a minimum age of 329.6 ± 1.1 Ma, interpreted as a maximum age for argon closure in this sample. A younger than 329 Ma date for this sample is compatible with hornblende dates for other Inner Piedmont rocks, reported in Steltenpohl and Kunk (1993), that range from younger than 322 Ma to 320 Ma.

Muscovite sample GW-l is from the type 1 mylonitized, K-feldspar–rich pegmatite body within the Goodwater-Enitachopco fault depicted in Figure 3 (see Figs. 2 and 10). Muscovite fish separated from this sample were as long as 6 mm and were derived from retrograde shearing of earlier formed larger grains. Because microstructures indicate medium-grade conditions for shearing between 450 and 600 °C (Passchier and Trouw, 1996), we interpret the 327.4 ± 1.6 Ma plateau age as the time of cooling through muscovite closure (~350 °C) following type 1 mylonitization. This date is very close to the ca. 334 Ma date for the Mitchell Dam hornblende sample (MD-1). Two possible explanations are that projection of the ca. 334 Ma date into the line of the profile in Figure 11 is not justifiable, or this part of the eastern Blue Ridge cooled very quickly from ~500 to ~350 °C between 333 and 329 Ma (respectively, for hornblende and muscovite closure). Additional $^{40}Ar/^{39}Ar$ dates are needed to evaluate this relationship. The middle Mississippian date for muscovite sample GW-1 is interpreted to place a minimum on the time of type 1 shearing along Goodwater-Enitachopco fault.

TABLE 1. SAMPLE LOCALITIES

Samples	Terrane	Rock or unit	Location (latitude, longitude)
MD-1	Eastern Blue Ridge	Mitchell Dam Amphibolite	32°48.10′N, 86°25.90′W
GW-1	Eastern Blue Ridge	Unnamed pegmatite	33°3.88′N, 86°3.13′W
GE-1, 10ENITA1	Eastern Blue Ridge	Trondhjemite dike	33°2.15′N, 86°7.28′W
Elk-21	Eastern Blue Ridge	Trondhjemite dike	32°54.09′N, 85°59.68′W
AL-49	Inner Piedmont	Ropes Creek Amphibolite	32°43.66′N, 85°47.19′W

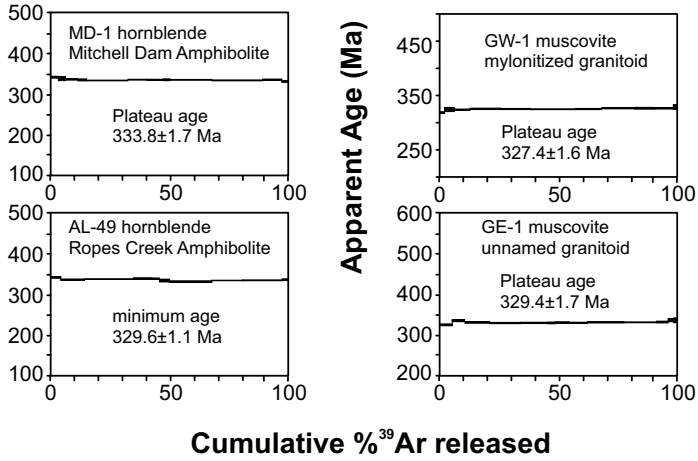

Figure 10. The $^{40}Ar/^{39}Ar$ step-heating analyses from select rocks of the study area (see text).

Muscovite sample GE-l (Figs. 2 and 10) is from the tabular, <3-m-thick, prekinematic trondhjemite injection within the type 2 Goodwater-Enitachopco shear zone shown in Figure 5A; muscovite was separated from the same altered sample in Figure 6A. The 329 ± 1.7 Ma plateau age is within analytical uncertainty of the muscovite age determined for sample GW-1. This age could record either the time of closure following cooling from metamorphism or from cooling after fluid-assisted shearing along the Goodwater-Enitachopco fault.

These $^{40}Ar/^{39}Ar$ dates support late Mississippian exhumation and cooling in this part of the eastern Blue Ridge. Figure 11 provides their context with respect to what is known about the mineral cooling architecture along the general transect depicted in Figure 1. From northwest to southeast, McClellan et al. (2007) reported dates from the Talladega slate belt that are only slightly younger than those that we report for the eastern Blue Ridge. Assuming normal upright cooling prior to fault movement, this is compatible with only minor top-down-to-the-southeast normal fault motion along the Goodwater-Enitachopco fault because older already cooled isothermal surfaces appear to have been brought downward in the hanging-wall block. Steltenpohl and Kunk (1993) and Steltenpohl et al. (2004a) report data from the Inner Piedmont eastward across the Pine Mountain basement-cover massif to where the Uchee terrane is covered by the coastal plain onlap. Mineral cooling dates from the Inner Piedmont directly southeast of the Brevard zone are generally similar to those of the eastern Blue Ridge. Farther southeast, cooling dates drop dramatically as the border fault with the Pine Mountain window (Towaliga fault) is approached. Rocks of the Pine Mountain window and the Uchee terrane represent the deep-seated late Alleghanian metamorphic core, where peak uppermost amphibolite to near granulite facies conditions (Chalokwu, 1989) were attained as late as ca. 288 Ma (Steltenpohl and Kunk, 1993; Steltenpohl et al., 2004b, 2008, 2010). In Steltenpohl and Kunk (1993), the pronounced discordance in cooling dates associated with the Towaliga fault was interpreted to reflect substantial top-down-to-the-west normal fault displacement of the isothermal surfaces. Geometry, kinematics, and mineral cooling architecture therefore suggest that the Goodwater-Enitachopco and Towaliga faults may frame a large graben-like structure. However, the time of movement along either fault system is not known precisely enough to speculate on whether they are part of the same system of faults. In addition, flow into and out of the line of section likely was substantial, as evidenced by the presence of major strike-slip faults, further complicating interpretations of the resultant mineral cooling patterns.

U-Pb Analyses and Their Interpretation

We analyzed U-Pb isotopes in zircons from two trondhjemite dikes, one that cuts the metamorphic foliation and dextral shears within the Elkahatchee Quartz Diorite, and one that had intruded prior to movement along the Goodwater-Enitachopco fault (see Fig. 2, sample localities 4 and 2, respectively). In the Elkahatchee exposure, narrow (<0.5 m thick), steeply dipping trondhjemitic dikes cut across the dextral shear zones at high angles (Fig. 9A). The dikes are lighter gray colored and finer grained than the quartz diorite. Metamorphic foliation within the dikes appears to be coplanar with that observed in the Elkahatchee Quartz Diorite, although the fabric is not as strongly developed in the dikes (see also Moore et al., 1987). We analyzed U-Pb isotopes of zircons separated from the trondhjemite dike shown in Figure 9A (Elk-21) where it cuts across several of the right-slip shears; 16 U-Pb analyses from sample Elk-21 were performed on whole single grains, individual parts broken from a single grain, and small multigrain fractions (Fig. 12A; Table 2). Five samples with the youngest $^{207}Pb/^{206}Pb$ ages define a linear array with a slightly elevated MSWD (mean square of weighted deviates) of 1.7 (Fig. 12A); 11 other fractions plot

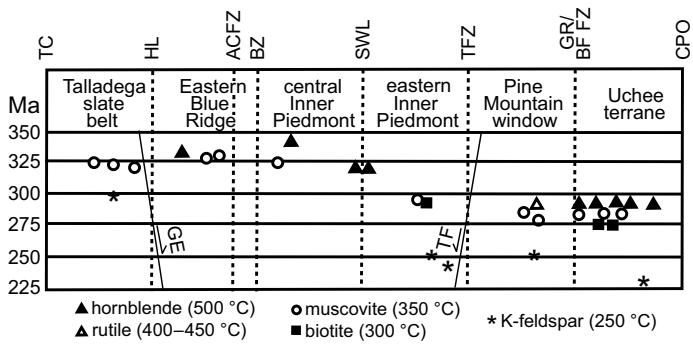

Figure 11. Synoptic diagram illustrating thermochronological constraints along the general profile shown in Figure 1. Horizontal axis is approximate geographic position. Vertical axis is mega-annum (Ma–million years). Legend indicates all are $^{40}Ar/^{39}Ar$ cooling dates except for the U-Pb date on rutile; general closing temperatures are presented parenthetically. Abbreviations are as in Figure 1 (CPO—Coastal Plain onlap; TFZ—Towaliga fault zone; TF—Towaliga fault). Data are ours and from Steltenpohl and Kunk (1993), Steltenpohl et al. (2004b), and McClellan et al. (2007).

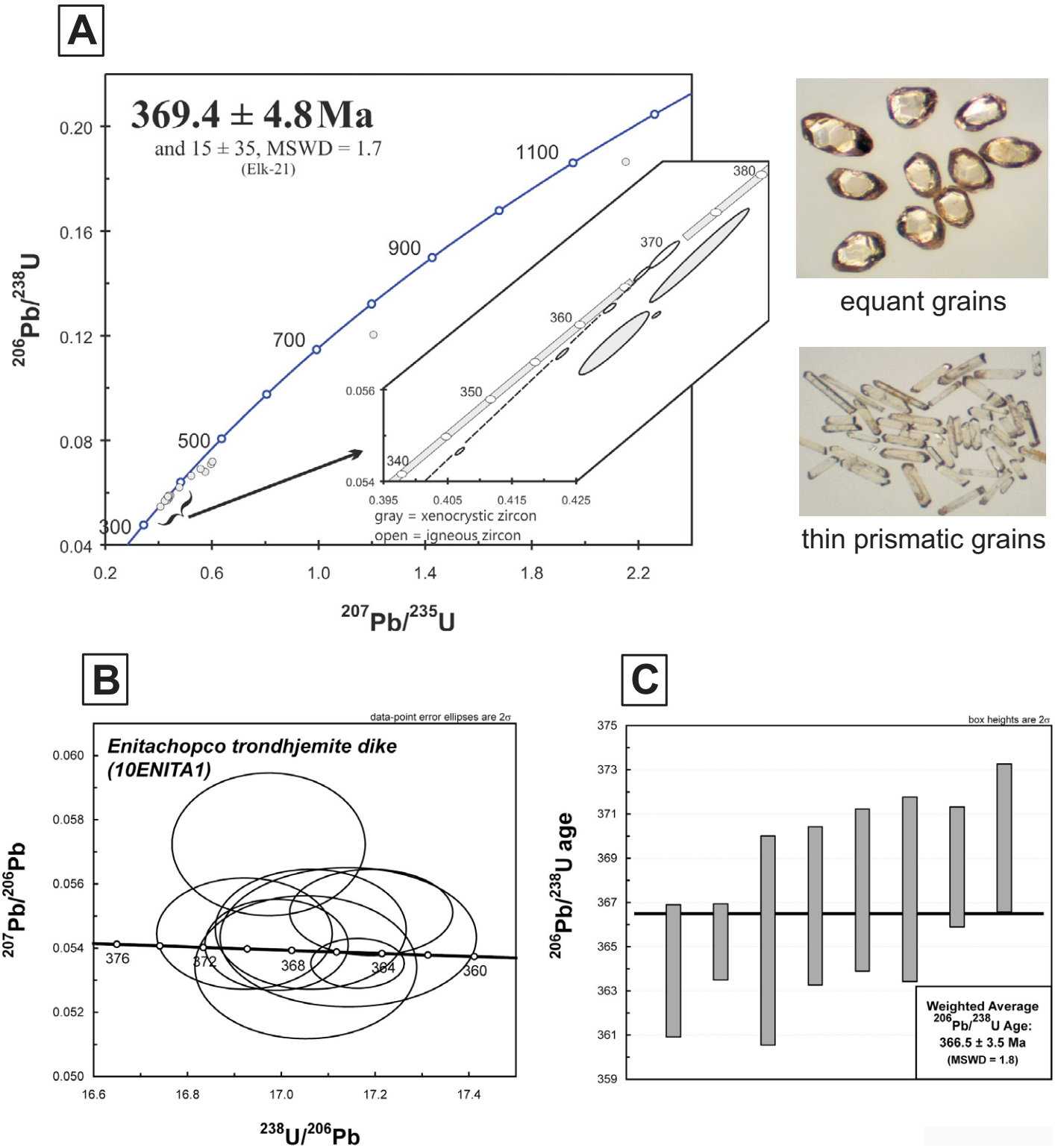

Figure 12. U-Pb isotopic results. (A) Conventional U-Pb concordia diagram for zircon grains from trondhjemite dike sample Elk-21 that intrudes the Elkahatchee Quartz Diorite (MSWD—mean square of weighted deviates). Error envelopes for expanded view are 2σ. Inset photomicrographs (original photo widths = 1.2 mm) of equant and squat prisms (significant inherited components) and thin prismatic grains (some had inherited components that others did not; see Table 3). (B) Tera-Wasserburg concordia plot of U-Pb SHRIMP (sensitive high-resolution ion microprobe–reverse geometry) data from zircons extracted from sample 10ENITA1, from a prekinematic trondhjemite dike within a type 2 shear zone of the Goodwater-Enitachopco fault. Error envelopes are 2σ. (C) Age ranges for eight zircons analyzed from 10ENITA1; mean = 366.5 ± 3.5 Ma, MSWD = 1.8 (error bars are 2σ).

TABLE 2. U-Pb ISOTOPIC DATA FOR ELK-21

Sample/Fraction (number of grains)	Weight (mg)*	Total* U (ng)	Total† Pb (pg)	Total† common Pb (pg)	U (ppm)	P (ppm)	Atomic ratios							Ages (Ma)			Corr.** coeff.
							$^{206}Pb/^{204}Pb$†	$^{206}Pb/^{208}Pb$§	$^{206}Pb/^{238}U$§	Error# (%)	$^{207}Pb/^{235}U$§	Error# (%)	$^{207}Pb/^{206}Pb$§	Error# (%)	$^{206}Pb/^{238}U$	$^{207}Pb/^{235}U$	$^{207}Pb/^{206}Pb$	
Elk-21																		
Squat prism (1)	0.025	0.62	121.6	1.47	25	5	5001	0.1467	0.18644	0.468	2.15235	0.474	0.08373	0.076	1102.0	1165.8	1286.3	0.99
Medium equant (3)	0.044	2021	264.0	3.44	50	6	4940	0.0828	0.12040	0.229	1.20590	0.240	0.07264	0.071	732.9	803.3	1003.9	0.96
Tiny flat hexagons (8)	0.052	30786	254.3	1.13	72	5	14394	0.0953	0.06800	0.225	0.57483	0.234	0.06131	0.063	424.1	461.1	650.2	0.96
Large tip (1)	0.018	5.14	349.1	1.67	285	19	13913	0.0545	0.07088	0.188	0.59636	0.211	0.06103	0.093	441.4	474.9	640.2	0.90
Large prism (1)	0.020	3.22	223.4	1.49	161	11	9918	0.0603	0.07188	0.166	0.60156	0.182	0.06070	0.073	447.5	478.2	628.5	0.92
Large equant (1)	0.022	2.51	164.5	2.38	114	7	4656	0.0468	0.06907	0.285	0.55700	0.311	0.05848	0.121	430.6	449.6	548.0	0.92
Medium prisms (3)	0.068	0.35	24.5	1.64	5	0	923	0.1676	0.06641	2.140	0.52230	2.225	0.05704	0.577	414.5	426.7	493.2	0.97
Large metamict (1)	0.031	35.5	2590	8.89	1146	84	15804	0.3091	0.06203	0.074	0.47777	0.099	0.05586	0.066	387.9	396.5	447.0	0.75
Small tips (3)	0.022	5.25	279.4	1.27	239	13	15179	0.0190	0.05764	0.100	0.43744	0.120	0.05504	0.066	361.3	368.4	413.9	0.84
Thin prism (1)	0.015	0.31	17.4	1.28	20	1	892	0.0979	0.05703	0.980	0.43082	1.044	0.05479	0.346	357.5	363.8	403.8	0.94
Thin prism (1)	0.015	0.58	35.1	1.72	39	2	1291	0.1355	0.05893	1.405	0.44424	1.429	0.05468	0.255	369.1	373.2	399.0	0.98
Thin prisms (8)	0.125	2.91	172.4	1.27	23	1	8429	0.1390	0.05779	0.152	0.43013	0.183	0.05399	0.102	362.1	363.3	370.4	0.83
Thin prism (1)	0.022	0.93	52.7	1.90	42	2	1847	0.0694	0.05894	0.405	0.43869	0.435	0.05398	0.153	369.2	369.3	370.1	0.94
Large thin prism (1)	0.020	2.79	157.6	1.00	140	8	10071	0.1015	0.05680	0.169	0.42266	0.187	0.05397	0.077	356.1	357.9	369.8	0.91
Fat prism (1)	0.025	2.39	131.1	1.51	96	5	5905	0.0371	0.05853	0.220	0.43517	0.235	0.05393	0.080	366.7	366.8	368.0	0.94
Tips (2)	0.022	4.57	231.2	1.34	208	11	11865	0.0229	0.05469	0.119	0.40664	0.141	0.05393	0.076	343.3	346.5	368.0	0.84

*Weight estimated from measured grain dimensions and assuming density = 4.67g/cm^3, ~25% uncertainty affects only U and Pb concentrations.
†Corrected for fractionation (0.18% ± 0.09%/amu – Daly) and spike.
§Corrected for fractionation, blank, and initial common Pb.
#Errors are 2σ.
**$^{207}Pb/^{235}U$ – $^{206}Pb/^{238}U$ correlation coefficient of Ludwig (1989).

significantly to the right of this array, likely due to inherited older zircon. The two oldest of these analyses suggest a component of Mesoproterozoic inherited material. The five youngest analyses consist of both single-grain and multigrain fractions of prismatic zircon grains, including two tips broken from prismatic grains. A discordia cord fit through these five analyses yields an upper intercept of 369.4 ± 4.8 Ma. We interpret this age to mark the time of crystallization of the dike from which Elk-21 was sampled.

We also analyzed zircons from sample 10ENITA1 (sample locality 2 in Fig. 2; for analyses, see Table 3) collected from the prekinematic trondhjemite dike within the type 2 Goodwater-Enitachopco shear zone shown in Figure 5A ($^{40}Ar/^{39}Ar$ sample GE-1 is from this same dike). We interpret this prekinematic dike to have originally intruded with a relatively steep dip, making a high angle to the host rock compositional layering and metamorphic foliation, similar to the Elkahatchee dike from which Elk-21 was sampled (e.g., Fig. 9A). Zircons from the dike are highly complex; nearly all grains contain low uranium, xenocrystic cores mantled by higher uranium interior and rim domains (Figs. 12B, 12C). Core domains are often irregular and embayed, suggesting resorption of preexisting zircon. Interior and rim domains are volumetrically most significant and display weak oscillatory zoning. Individual spot analyses (n = 8) from zircon interior and rim domains yielded an error-weighted average $^{206}Pb/^{238}U$ age of 366.5 ± 3.5 Ma (MSWD = 1.8) (Figs. 12B, 12C). We interpret this age to mark the time of crystallization of the dike from which 10ENITA1 was sampled.

Our 369 Ma U-Pb zircon date on the Elk-21 dike sample provides a minimum age of igneous crystallization of the Elkahatchee Quartz Diorite; the maximum age is loosely constrained by the ca. 388–370 Ma range of zircon ages reported by P.M. Mueller (2010, personal commun.), who stated that the dates are "messy" and more work needs to be done to better constrain the age. The excellent preservation of crosscutting relationships exposed at the Elk-21 sample locality also allows for bracketing the timing of the metamorphic fabric in the Elkahatchee to between ca. 388 and 369 Ma; the coplanar fabric preserved in the dike, however, suggests that metamorphic strains continued beyond 369 Ma, which is consistent with regional evidence for early and late Alleghanian metamorphism in rocks of the Alabama Piedmont (Steltenpohl and Kunk, 1993; Gastaldo et al., 1993; McClellan et al., 2007; Steltenpohl et al., 2008). Because the dike also cuts shear zones that cut the metamorphic foliation, the 369 Ma date places a minimum on the age of right-slip shearing. The

TABLE 3. U-Pb SHRIMP ISOTOPIC ANALYSES AND AGES FOR 10ENITA1

Grain	Concentrations U (ppm)	Th (ppm)	Th/U	Pb*	f206† (%)	Atomic ratios 238U/206Pb§	Error (%, 1σ)	207Pb/206Pb§	Error (%, 1σ)	206Pb/238U**	Error (absolute, 1σ)	Average age 206Pb/238U††	Error (absolute, 1σ)	Weighted average age (2σ)
Enitachopco prekinematic biotite-muscovite trondhjemite dike														
10ENITA1	3832.96	37.53	0.0097925	191.87	–0.04	17.16	0.24	0.0535	0.59	0.05829	0.0001	365.22	0.86	66.5 ± 3.5 Ma
10ENITA1	990.32	3.85	0.0038889	50.08	0.02	16.99	0.37	0.0541	1.07	0.05885	0.0002	368.61	1.36	
10ENITA1	631.37	14.50	0.0229638	32.05	0.06	16.92	0.45	0.0545	1.30	0.05906	0.0003	369.91	1.67	
10ENITA1	392.82	5.84	0.0148604	19.69	0.06	17.14	0.65	0.0543	1.63	0.05830	0.0004	365.28	2.37	
10ENITA1	381.02	9.76	0.0256126	19.20	–0.06	17.05	0.57	0.0534	1.70	0.05868	0.0003	367.60	2.08	
10ENITA1	528.26	13.45	0.0254628	26.60	0.09	17.06	0.49	0.0546	1.40	0.05856	0.0003	366.85	1.79	
10ENITA1	976.34	26.75	0.0274032	48.79	0.16	17.19	0.41	0.0551	0.99	0.05807	0.0002	363.91	1.50	
10ENITA1	543.65	8.73	0.0160495	27.52	0.41	16.97	0.50	0.0572	1.59	0.05867	0.0003	367.56	1.84	

Note: Atomic ratio errors are reported at 1σ level and refer to last digits.
*Radiogenic ^{206}Pb.
†Fraction of total ^{206}Pb that is common ^{206}Pb.
§Uncorrected ratios.
**^{206}Pb corrected ratios using age-appropriate Pb isotopic composition of Stacey and Kramers (1975).
††^{207}Pb corrected age.

367 Ma zircon age for dike sample 10ENITA1 overlaps with analytical uncertainty our date on sample Elk-21, suggesting that similar appearing dikes across the eastern Blue Ridge in Alabama and western Georgia may be part of a swarm of dikes intruded in the Late Devonian. Our date also places a maximum on the age of movement along the type 2 Goodwater-Enitachopco shear zones.

DISCUSSION

Our work in the Alabama and Georgia Blue Ridge was aimed at exploring the structural and temporal transition between late Paleozoic contraction in the foreland and apparently synchronous right-slip shearing in the hinterland, but three key findings were unexpected: (1) some right-slip shear zones marginal to the Alexander City fault formed during the Devonian; (2) the right-slip Alexander City fault zone is overprinted and locally excised by high-angle brittle faults; and (3) the Goodwater-Enitachopco is a sub–ductile-brittle transition oblique-dextral-normal-slip fault exposed far toward the foreland. These findings do not conform to current interpretations of the tectonic evolution of the southernmost Appalachians, and we explore their possible explanations and significance in the following.

Devonian Dextral Shears in Alexander City Fault Zone Shoulder Rocks

Devonian right-lateral strike-slip shearing of the Elkahatchee Quartz Diorite establishes that Neoacadian dextral shearing had already occurred in rocks of the eastern Blue Ridge ~40 m.y. before movement had initiated along the system of Carboniferous (Alleghanian) dextral shear zones (Secor et al., 1986). Late Devonian dextral shearing is reported in more northern parts of the southern Appalachian Blue Ridge (Ferrill and Thomas, 1988; Trupe et al., 2003; Hatcher, 2010), but the dextral shears in the Elkahatchee are the first to be documented from the orogen's most southern surface exposures. Geological investigations in the eastern Blue Ridge of western North Carolina led workers to suggest the presence of a system of Devonian dextral transform faults in that area (see Adams et al., 1996; Trupe et al., 2003). Trupe et al. (2003) recognized the Burnsville fault (Fig. 1) as a fundamental right-slip fault within this system, and dated its movement to between 377 and 373 Ma. Similar kinematics, geometries, and now timing suggest that the Devonian dextral shears in the Alabama Blue Ridge might be related to the Burnsville dextral shear system. However, Trupe et al. (2003) had difficulties reconciling the southwestern continuation of the Burnsville fault (see question mark in Fig. 1), and they posed two hypotheses: (1) the Burnsville fault links with the Neoacadian Dahlonega-Chattahoochee shear zone, and (2) the Burnsville fault is cut by the later-formed Alleghanian faults. The most proximal major dextral shear zone to the ca. 388–369 Ma Elkahatchee shears is the Alexander City fault (Fig. 2), but the latter is a lower temperature retrograde mylonite zone that most likely overprinted the former shears. Movement along the Alexander City fault zone therefore likely postdated 369 Ma. Workers have generally speculated that the Alexander City fault is a Carboniferous structure, given its similarities with other Alleghanian dextral shear zones (Guthrie, 1995; Steltenpohl et al. 1996), and this is compatible with the mineral cooling data presented in Figure 11. Future mapping and structural studies are needed to determine how the high-temperature Devonian mylonites relate to the Alexander City fault. The fault zone might be a polyphase structure like the Brevard zone, with a Neoacadian movement history that predated Alleghanian reactivation during dextral shearing.

High-Angle Brittle Fault Overprinting of the Alexander City Fault

Brittle faults, cataclasites, and cataclastic pods associated with the Alexander City fault zone resemble those that are reported for the Towaliga fault along the northwest margin of the Pine Mountain window in eastern Alabama and central Georgia (see Fig. 1 for location: Babaie et al., 1991; Hadizadeh et al., 1991; Steltenpohl, 1992; Steltenpohl et al., 2010; Huebner and Hatcher, 2011). They are also very similar to brittle faults in parts of the Blue Ridge and Inner Piedmont of North and South Carolina (Garihan and Ranson, 1992; Garihan et al., 1993). All are interpreted to be post-Appalachian and related to the Mesozoic rifting of Pangea. We interpret that the brittle faults cutting the Alexander City fault have drastically thinned the zone of mylonites and phyllonites to the point that locally it is completely excised. The style of interplay and reactivation is particularly reminiscent of the brittle faults that overprint the sub–ductile-brittle transition Towaliga mylonite zone (Huebner et al., 2010; Steltenpohl et al., 2010). Huebner and Hatcher (2011) interpreted silicified cataclastic pods along the Towaliga mylonite zone to have formed as dilational stepovers during later supra–ductile-brittle transition reactivation and inversion of right-slip movement. Although this might explain how some of the siliceous pods formed along the Alexander City fault zone, at least one of the pods

contains a 7-m-thick, 20-m-long section of layered orthoquartzite instead of injected quartz. The affinity of this orthoquartzite is unknown, but it resembles those found in the Jacksons Gap Group of the Brevard zone (Wielchowsky, 1983; Sterling et al., 2005; Sterling, 2006), suggesting that it might have been transferred westward along a splay fault connecting the two fault zones. Regardless of the precise mode of their formation, the brittle faults along the Towaliga combine with our findings along the Alexander City fault zone to suggest a broad graben-like structure between them (Fig. 13A). Although the timing of brittle movement is not yet precisely known to establish a link between them, the rheological and petrological similarities are compatible with such an interpretation.

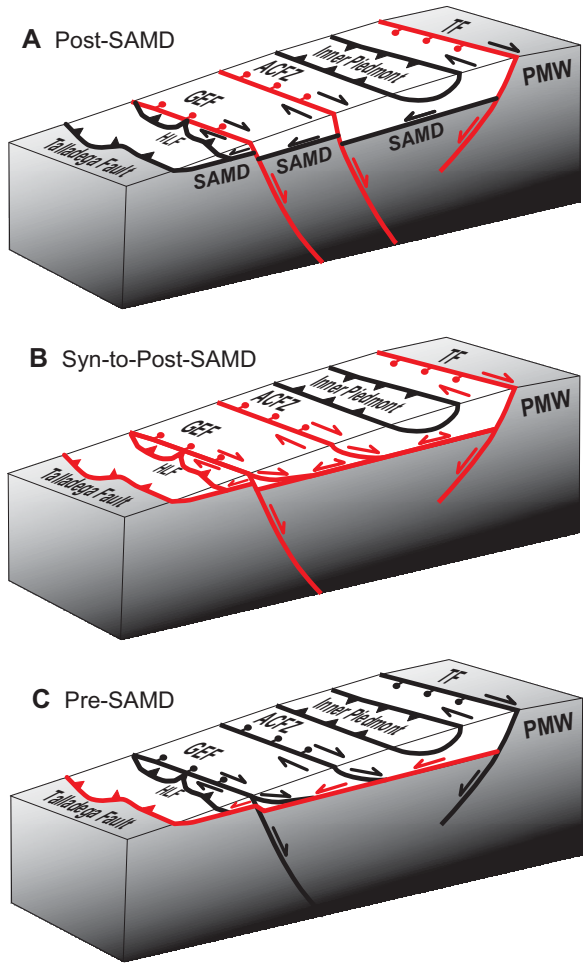

Figure 13. Block diagrams (northwest is to the left) illustrating hypothetical scenarios for the evolution of extensional and select contractional faults as framed temporally around movement along the southern Appalachian master décollement (SAMD). Red lines indicate active faults. ACFZ—Alexander City fault zone; GEF—Goodwater-Enitachopco fault; HLF—Hollins Line fault; PMW—Pine Mountain window; TF—Towaliga fault. (A) Post-SAMD. Triassic–Jurassic rifting of Pangea. (B) Syn-SAMD to post-SAMD. Permian–Triassic collapse of the Alleghanian orogen. The double barbed symbols along the SAMD imply combinations of contraction and extension (see text). (C) Pre-SAMD. Late Carboniferous–Early Permian extension.

Extensional Tectonics in the Southernmost Appalachians

Top-to-the-south-southeast normal-slip movement along the Goodwater-Enitachopco fault is unusual, particularly considering its position far toward the foreland. There are still no absolute timing constraints on the fault (between the late Carboniferous and Early Jurassic), and in the following we frame our discussion around its movement relative to that along the southern Appalachian master décollement (Cook et al., 1979), which is broadly accepted as the final contractional phase of the Alleghanian orogeny (latest Pennsylvanian to earliest Permian: Hatcher, 1987, 1989, 2002, 2010). Figure 13 illustrates three possible scenarios: (1) post–southern Appalachian master décollement (Triassic–Jurassic) rifting of Pangea; (2) synchronous to post–southern Appalachian master décollement (Permian–Triassic) collapse of the thickened Alleghanian orogenic welt; and (3) pre–southern Appalachian master décollement extension.

At first glance it would appear that normal-slip movement along the Goodwater-Enitachopco fault was associated with the Mesozoic rifting of Pangea (Fig. 13A), a fundamental and well-known period of extension expressed along the entire eastern seaboard of North America. The Blue Ridge is to the northwest of the zone most directly affected by Mesozoic extension (Klitgord et al., 1988), however, and the Goodwater-Enitachopco fault would be the orogen's most forelandward Triassic–Jurassic rift fault. Several lines of evidence seem contrary to this interpretation. (1) It would seem that other typical expressions of Mesozoic rifting should be prevalent in this area, but no diabase dikes occur within the entire region shown in Figure 2, and the closest rift basin is beneath the Gulf of Mexico coastal plain several hundred kilometers south of our area. However, border faults in the Red Sea rift occur outside the locus of magmatic activity (see Keranen and Klemperer, 2008), and the Mesozoic landscape in this part of the southern Appalachians has been deeply eroded, so any shallow-level intrusions, volcanics, or sedimentary deposits might have been eroded away. (2) The sub–ductile-brittle transition level of formation of the Goodwater-Enitachopco fault is in stark contrast to the supra–ductile-brittle transition faults that typify exposed Mesozoic rift faults in the Appalachians. (3) One would expect to find some record of Mesozoic disturbance in $^{40}Ar/^{39}Ar$ mineral cooling data from across the fault (e.g., Atekwana, 1987), but data (Fig. 11) do not indicate substantial normal-slip displacement of the ~350 °C paleoisothermal surface. (4) The persistent right-slip component documented for the type 2 Goodwater-Enitachopco shear zones conflicts with a purely extensional rift fault; such movement might be compatible, however, with Late Permian through Early Jurassic counterclockwise rotation of the Yucatan block out from the area of the Mississippi embayment as the Gulf of Mexico opened (Pindell and Dewey, 1982; Salvador, 1991; Pindell et al., 2000; Steiner, 2005). (5) Post-Alleghanian normal-slip movement along the Goodwater-Enitachopco would require it to cut entirely across the stack of Appalachian allochthons and across the décollement (Fig. 13A). The simplified cross section shown in Figure 2 illustrates that the Goodwater-Enitachopco fault is precisely above a basement step up interpreted as a Cambrian rift fault formed along the ancient Laurentian margin (Thomas and Neathery, 1980; Thomas et al., 1989; Thomas, 1991). Our surface observations therefore may indicate post-Alleghanian normal-fault reactivation of an earlier (Cambrian) rift fault. In Figure 13A the Towaliga fault is depicted as a Mesozoic rift fault (Nelson et al., 1987; Steltenpohl et al., 2010), and we suggest that the brittle overprinting of the Alexander City fault may likewise have offset the basement and the décollement. Seismic and core data do not indicate such a basement fault at the position of the Alexander City fault (e.g., Thomas et al., 1989; Thomas, 1991), but aeromagnetic data have been argued to suggest this possibility (Bajgain,

2011). Mesozoic reactivation of a Laurentian rift fault by the Goodwater-Enitachopco fault would further support the influence of tectonic inheritance on the evolution of eastern North America, punctuating the start and finish of two Wilson cycles (Hatcher, 1978, 1987, 2004, 2010; Thomas, 2006; Steltenpohl et al., 2010).

Orogenic collapse (e.g., Burchfiel and Royden, 1985; Dewey, 1988; Schwartz, 1988; Mercier et al., 1992; McNulty et al., 1998) provides an attractive alternative explanation for the Goodwater-Enitachopco fault (Fig. 13B). Its forelandward position and hinterland-directed movement is compatible with it having formed as the result of free-boundary collapse (Selverstone, 2005). Far-field effects, such as the opening of a continental rift, are known to control hinterland-directed extension in collapsing orogens (Fossen, 1992, 2000, 2010; Andersen, 1993), and such a setting had evolved south of our study area during the Mesozoic as the Gulf of Mexico began to open. As northwest-southeast contraction waned along the décollement, the thickened upper plate may have become free to translate south-southeastward. Such a case is reported for the Devonian extensional collapse of the Scandinavian Caledonides, where east-directed (Silurian–Devonian) thrust faults in the Swedish foreland were reactivated and reversed by top-to-the-west, hinterland-directed, normal-slip shears (i.e., back sliding; Fossen, 1992, 2000; Steltenpohl et al., 2004a, 2011). The backslid shear zones in Norway are cut by steeper dipping top-to-the-west normal faults that locally excise the lower angle shears, which is reminiscent of the type 1 and type 2 shears of the Goodwater-Enitachopco fault (Fig. 13B). Such steep-on-shallow overprinting also typifies western U.S. Cordilleran–style extensional faults, as the earlier formed crystal-plastic shear zones were progressively unroofed by brittle extensional faults to shallower crustal levels (Coney, 1980; Armstrong, 1982; Wernicke, 1985). The Goodwater-Enitachopco fault might therefore represent the breakaway fault to a Mesozoic extensional detachment system into which other faults had rooted, which is diagrammatically suggested in Figure 13B. Alternatively, fixed-boundary collapse might explain extensional movement along the Goodwater-Enitachopco fault if it were synchronous with, and coupled to, contraction along on the décollement, similar to that reported for the South Tibetan detachment system and the Main Central thrust, respectively, in the active Himalayan orogen (Burchfiel and Royden, 1985; Burchfiel et al., 1992; Hodges et al., 1992). The oblique right-slip component on the Goodwater-Enitachopco, however, might also be explained by collapse and extrusion toward a free-lateral boundary located toward the southwest during synchronous convergence and orogen-parallel movement along the Alleghanian dextral shear system.

Several lines of evidence suggest that the Goodwater-Enitachopco fault might have initiated movement while positioned somewhere farther outboard, and was transported westward by the underlying décollement (Fig. 13C). For example, trondhjemite dikes that appear to have been injected synchronously with normal-slip shearing (e.g., Fig. 6D) have no counterparts associated with Mesozoic rifting (Guthrie and Raymond, 1992), but they could relate to the suite of early Alleghanian (ca. 350–330 Ma) trondhjemites. If fluid-assisted alteration of sample GE-1 accompanied normal-slip shearing along the Goodwater-Enitachopco fault, it could have rejuvenated the argon isotopic system in muscovite and resulted in the plateau age of 329 Ma (Fig. 10). Most paradoxical, however, are the sub–ductile-brittle transition fault rocks of the Goodwater-Enitachopco fault that formed at deeper crustal levels than is typical of Mesozoic rift faults exposed elsewhere in the eastern United States, and at least as deep as the thrust faults that underlie them, including the décollement (i.e., Talladega-Cartersville fault). The Goodwater-Enitachopco fault might therefore record extension prior to Alleghanian collapse, perhaps recording the final stages of orogen-parallel channelized flow in the middle crust (Merschat et al., 2005; Hatcher and Merschat, 2006) or some other event not yet understood. A lower age on the timing of such an event would be limited by the age of youngest Pennsylvanian strata cut in the footwall block (Tull, 1984), which is not precisely known (early to middle Pennsylvanian, between ca. 320 and 307 Ma; Hewitt, 1984).

CONCLUSIONS

Right-slip shear components observed for the Alexander City and Goodwater-Enitachopco faults indicate that the Alleghanian dextral shear system persists across the entire eastern Blue Ridge of Alabama and western Georgia. Right-slip motion along the Goodwater-Enitachopco fault likely was linked to the directly underlying Hollins Line dextral transpressional duplex, which would further extend the dextral shear system to the boundary with the western Blue Ridge. The geometries and kinematics of the Goodwater-Enitachopco fault and the Millerville generation cross-folds (Fig. 2) are compatible with them having formed synchronously with dextral transpressive movement along the Hollins Line duplex. Synchronous development might explain (1) why the Goodwater-Enitachopco fault is best developed along the crest of the Millerville antiform, where decoupling may have accommodated cross-folding of the footwall block, (2) the similar rheologies of the Goodwater-Enitachopco and the Hollins Line mylonites, and (3) the restricted occurrence of the cross-folds (Fig. 2) along the frontal crystalline thrusts in this region (Tull, 1984). The cross-folds may therefore record mild dextral transpressional strains that propagated into the Valley and Ridge along the Talladega-Cartersville fault. Partitioning between dextral and contractional strains in Alabama and western Georgia thus sharply contrasts with that reported northeast of the Cartersville transform. In Figure 1 we project the Cartersville transform to extend to the eastern terminus of the Pine Mountain window, implying that it marks a surface exposure of the southwest step up of the subdécollement basement. Steltenpohl et al. (1992, 2008) reported that latest Pennsylvanian to earliest Permian right-slip movement along fundamental mylonite zones flanking the Pine Mountain window overlapped in time with thrusting along the décollement. The Cartersville transform therefore appears to have formed a lateral buttress (ramp) that forced the décollement to climb obliquely out of the Tennessee embayment onto the Alabama promontory (Fig. 1; Tull et al., 1998a, 1998b; Tull and Holm, 2005; Thomas and Steltenpohl, 2010), explaining the local decapitation of folds in the Talladega-Cartersville footwall block. This interpretation also is compatible with geologic observations from the Pine Mountain window that suggest the décollement was abandoned or otherwise redirected to another structural level as it impinged the distal Laurentian continental margin (Hooper et al., 1997; McBride et al., 2005; Steltenpohl et al., 2010).

The Cartersville transform also appears to have had influence on the late to post-Appalachian extensional evolution of the orogen, given that normal faults like the Goodwater-Enitachopco are not reported northeast of it. The loose late Carboniferous to Early Jurassic timing constraints for normal-slip movement along the Goodwater-Enitachopco fault leave plenty of room for interpretation, but we favor the following. Late Alleghanian convergence along the décollement progressively thickened rocks of the Blue Ridge, eventually creating a steep northwest-facing (present-day direction) mountain front. Topography grew with continued movement along the décollement until the upper parts of this crustal wedge became gravitationally unstable, triggering southeast-directed extensional movement on the Goodwater-Enitachopco fault. As the décollement impinged on the Cartersville transform, strains

were channeled obliquely along it, resulting in dextral transpression. Synchronous southwest-driven, orogen-parallel extrusion was accommodated along the deeper portions of the Alleghanian dextral shear system, contributing to the collapse of the orogen. Finally, rifting of Pangea during the Mesozoic reactivated some of the collapse structures and the Gulf of Mexico began to open.

ACKNOWLEDGMENTS

Acknowledgment for this research is made to the donors of the Petroleum Research Fund, administered by the American Chemical Society (ACS-PRF 23762-GB2 to Steltenpohl) and the U.S. Geological Survey Educational Mapping Program (Steltenpohl). Steltenpohl thanks the following Auburn University students who, through participating in various class projects, contributed to this research: Jake Ball, Dannena Bowman, Wes Buchanan, Geri Devilliers, Jennifer Glidewell, Jessica Horwitz, Thomas Key, Derick Unger, and John Hawkins. We thank a host of anonymous reviewers and associate editors who helped us to improve the manuscript.

REFERENCES CITED

Adams, M.G., Stewart, K.G., Trupe, C.H., and Willard, R.A., 1996, Tectonic significance of high-pressure metamorphic rocks and dextral strike-slip faulting in the southern Appalachians, *in* Hibbard, J.P., et al., eds., New perspectives in the Appalachian-Caledonian orogen: Geological Association of Canada Special Paper 41, p. 21–42.

Allison, D., 1992, Structural evolution and metamorphic petrogenesis of a metasediment and metaigneous complex, Coosa County, Alabama [Ph.D. thesis]: Tallahassee, Florida State University, 377 p.

Andersen, T.B., 1993, The role of extensional tectonics in the Caledonides of south Norway: Journal of Structural Geology, v. 15, p. 1379–1380, doi:10.1016/0191-8141(93)90114-P.

Armstrong, R., 1982, Cordilleran metamorphic core complexes—From Arizona to southern Canada: Annual Review of Earth and Planetary Sciences, v. 10, p. 129–154, doi:10.1146/annurev.ea.10.050182.001021.

Atekwana, E.A., 1987, $^{40}Ar/^{39}Ar$ thermochronology of the late Paleozoic Liberty Hill, Pageland and Lilesville plutons and the adjacent Wadesboro Mesozoic basin, North and South Carolina [M.S. thesis]: Washington, D.C., Howard University, 127 p.

Babaie, H.A., Hadizadeh, J., Babaie, A., and Ghazi, A.M., 1991, Timing and temperature of cataclastic deformation along segments of the Towaliga fault, western Georgia, U.S.A.: Journal of Structural Geology, v. 13, p. 579–586, doi:10.1016/0191-8141(91)90044-J.

Bajgain, S., 2011, Gravity and magnetic modeling of basement beneath Alabama Gulf Coastal Plain [M.S. thesis]: Auburn, Alabama, Auburn University, 88 p.

Barineau, C.I., 2009, Superposed fault systems of the southernmost Appalachian Talladega belt: Implications for Paleozoic orogenesis in the southern Appalachians [Ph.D. thesis]: Tallahassee, Florida State University, 150 p.

Bearce, D.N., 1979, Geology of the Talladega belt in the Hightower reentrant, Cleburne County, Alabama, *in* Tull, J.F., and Stow, S.H., eds., The Hillabee metavolcanic complex and associated rock sequences: Alabama Geological Society 17th Annual Field Trip Guidebook, p. 37–40.

Bentley, R.D., and Neathery, T.L., 1970, Geology of the Brevard fault zone and related rocks of the Inner Piedmont of Alabama: Alabama Geological Society 8th Annual Field Trip Guidebook, 119 p.

Bobyarchick, A.R., 1983, Structure of the Brevard zone and Blue Ridge near Lenoir, North Carolina, with observations on oblique crenulation cleavage and a preliminary theory for irrotational structures in shear zone [Ph.D. thesis]: Albany, State University of New York, 360 p.

Bobyarchick, A.R., 1999, The history of investigation of the Brevard fault zone and evolving concepts in tectonics: Southeastern Geology, v. 38, p. 223–238.

Bobyarchick, A.R., Edelman, S.H., and Horton, J.W., Jr., 1988, The role of dextral strike-slip in the displacement history of the Brevard zone, *in* Secor, D.T., Jr., ed., Southeastern geological excursions (Geological Society of America annual meeting field trip guidebook): Columbia, South Carolina Geological Survey, p. 53–104.

Bothner, W.A., and Hussey, A.M., II, 1999, Norumbega connections: Casco Bay, Maine, to Massachusetts?, *in* Ludman, A., and West, D.P., Jr., eds., Norumbega fault system in the northern Appalachians: Geological Society of America Special Paper 331, p. 59–72, doi:10.1130/0-8137-2331-0.59.

Bream, B.R., 2002, The southern Appalachian Inner Piedmont: New perspectives based on recent detailed geologic mapping, Nd isotopic evidence, and zircon geochronology, *in* Hatcher, R.D., Jr., and Bream, B.R., eds., Inner Piedmont geology in the South Mountains–Blue Ridge Foothills and the southwestern Brushy Mountains, central-western North Carolina: Annual field trip guidebook: Durham, North Carolina, Carolina Geological Society, p. 45–63.

Bream, B.R., 2003, Tectonic implications of para- and orthogneiss: Geochronology and geochemistry from the southern Appalachian crystalline core [Ph.D. thesis]: Knoxville, University of Tennessee, 296 p.

Burchfiel, B.C., and Royden, L.H., 1985, North-south extension within the convergent Himalayan region: Geology, v. 13, p. 679–682, doi:10.1130/0091-7613(1985)13<679:NEWTCH>2.0.CO;2.

Burchfiel, B.C., Chen, Z.L., Hodges, K.V., Liu, Y.P., Royden, L.H., Deng, C.R., and Xu, J.N., 1992, The South Tibetan detachment system, Himalayan Orogen: Extension contemporaneous with and parallel to shortening in a collisional mountain belt: Geological Society of America Special Paper 269, 41 p., doi:10.1130/SPE269.

Carrigan, C.W., Bream, B., Miller, C.F., and Hatcher, R.D., Jr., 2001, Ion microprobe analyses of zircon rims from the eastern Blue Ridge and Inner Piedmont, NCSC-GA: Implications for the timing of Paleozoic metamorphism in the southern Appalachians: Geological Society of America Abstracts with Programs, v. 33, p. 7.

Carter, B.T., Steltenpohl, M.G., and Andresen, A., 2001, Late-orogenic extension in the southernmost Appalachians compared with the northern Caledonides: A kinematic pattern of collapse?: Geological Society of America Abstracts with Programs, v. 33, no. 2, p. A-20.

Chalokwu, C.I., 1989, Epidote-amphibolite to amphibolite facies transition in the southern Appalachian Piedmont: P-T conditions across the garnet and calc-silicate isograds: Geology, v. 17, p. 491–494, doi:10.1130/0091-7613(1989)017<0491:EATAFT>2.3.CO;2.

Coney, P., 1980, Cordilleran metamorphic core complexes—An overview, *in* Crittenden, M., et al., eds., Cordilleran metamorphic core complexes: Geological Society of America Memoir 153, p. 7–31.

Cook, R.A., Albaugh, D.S., Brown, L.D., Kaufman, S., Oliver, J.E., and Hatcher, R.D., Jr., 1979, Thin-skinned tectonics in the crystalline southern Appalachians: COCORP seismic-reflection profiling of the Blue Ridge and Piedmont: Geology, v. 7, p. 563–568, doi:10.1130/0091-7613(1979)7<563:TTITCS>2.0.CO;2.

Cyphers, S.R., and Hatcher, R.D., Jr., 2006, The Chattahoochee-Holland mountain fault: A terrane boundary in the Blue Ridge of western North Carolina: Geological Society of America Abstracts with Programs, v. 38, no. 3, p. 66.

Dallmeyer, R.D., Wright, J., Secor, D.T., Jr., and Snoke, A., 1986, Character of the Alleghanian orogeny in the southern Appalachians: Part II. Geochronological constraints on the tectonic evolution of the eastern Piedmont in South Carolina: Geological Society of America Bulletin, v. 97, p. 1329–1344, doi:10.1130/0016-7606(1986)97<1329:COTAOI>2.0.CO;2.

Defant, M.J., 1980, A geochemical and petrogenetic analysis of the Almond and Blakes Ferry plutons, Randolph County, Alabama [M.S. thesis]: Tuscaloosa, University of Alabama, 118 p.

Defant, M.J., and Ragland, P.C., 1981, Petrochemistry of the trondhjemitic Almond and Blakes Ferry plutons, Randolph County, Alabama: Geological Society of America Abstracts with Programs, v. 13, p. 6.

Defant, M.J., Drummond, M.S., Arthur, J.D., and Ragland, P.C., 1987, The petrogenesis of the Blakes Ferry pluton, Randolph County, Alabama, *in* Drummond, M.S., and Green, N.L., eds., Granites of Alabama: Alabama Geological Survey Bulletin 128, p. 97–116.

Deininger, R.W., 1975, Granitic rocks in the northern Alabama Piedmont, *in* Neathery, T.L., and Tull, J.F., eds., Geologic profiles in the Northern Alabama Piedmont: Alabama Geological Society 13th Annual Field Trip Guidebook, p. 49–62.

Deininger, R.W., Neathery, T.L., and Bentley, R.D., 1973, Genetic relationships among granitic rocks in the northern Alabama Piedmont: Alabama Geological Survey Open-File Report, 18 p.

Dennis, A.J., and Secor, D.T., Jr., 1987, A model for the development of crenulations in shear zones with applications from the southern Appalachian Piedmont: Journal of Structural Geology, v. 9, p. 809–817, doi:10.1016/0191-8141(87)90082-4.

Dennis, A.J., and Wright, J.E., 1997, Middle and late Paleozoic monazite U-Pb ages, Inner Piedmont, South Carolina: Geological Society of America Abstracts with Programs, v. 29, no. 3, p. 12.

Dewey, J.F., 1988, Extensional collapse of orogens: Tectonics, v. 7, p. 1123–1139, doi:10.1029/TC007i006p01123.

Drummond, M.S., 1986, Igneous, metamorphic, and structural history of the Alabama Tin Belt, Coosa County, Alabama [Ph.D. thesis]: Tallahassee, Florida State University, 411 p.

Drummond, M.S., and Guthrie, G.M., 1986, Stratigraphy, metamorphism, and deformation of the northern Alabama Piedmont, *in* Whittington, D., et al., eds., Mineral resources of the northern Alabama Piedmont: Geological Society of America Southeastern Section Field Trip Guidebook: Tuscaloosa, Geological Survey of Alabama, p. 2–25.

Drummond, M.S., Allison, D.T., and Weslowski, D.J., 1994, Igneous petrogenesis and tectonic setting of the Elkahatchee Quartz Diorite, Alabama Appalachians: Implications for Penobscotian magmatism in the eastern Blue Ridge: American Journal of Science, v. 294, p. 173–236, doi:10.2475/ajs.294.2.173.

Drummond, M.S., Neilson, M.J., Allison, D.T., and Tull, J.F., 1997, Igneous petrogenesis and tectonic setting of granitic rocks from the eastern Blue Ridge and Inner Piedmont, Alabama Appalachians, *in* Sinha, A.K., et al., eds., The nature of magmatism in the Appalachian orogen: Geological Society of America Memoir 191, p. 147–164, doi:10.1130/0-8137-1191-6.147.

Ferrill, B.A., and Thomas, W.A., 1988, Acadian dextral transpression and synorogenic sedimentary successions in the Appalachians: Geology, v. 16, p. 604–608, doi:10.1130/0091-7613(1988)016<0604:ADTASS>2.3.CO;2.

Fossen, H., 1992, The role of extensional tectonics in the Caledonides of south Norway: Journal of Structural Geology, v. 14, p. 1033–1046, doi:10.1016/0191-8141(92)90034-T.

Fossen, H., 2000, Extensional tectonics in the Caledonides: Synorogenic or postorogenic?: Tectonics, v. 19, p. 213–224, doi:10.1029/1999TC900066.

Fossen, H., 2010, Extensional tectonics in the North Atlantic Caledonides: A regional view, *in* Law, R., et al., eds., Continental tectonics and mountain building: The legacy of Peach and Horne: Geological Society of London Special Publication 335, p. 767–793, doi:10.1144/SP335.31.

Garihan, J.M., and Ranson, W.A., 1992, Structure of the Mesozoic Marietta-Tryon graben, South Carolina and adjacent North Carolina, *in* Bartholomew, M.J., et al., eds., Basement tectonics 8: Characterization of ancient and Mesozoic continental margins—Proceedings of the 8th International Conference on Basement Tectonics, Butte, Montana, 1988: Dordrecht, Netherlands, Kluwer Academic Publishers, p. 539–555.

Garihan, J.M., Preddy, M.S., and Ranson, W.A., 1993, Summary of mid-Mesozoic brittle faulting in the Inner Piedmont and nearby Charlotte belt of the Carolinas, *in* Hatcher, R.D., Jr., and Davis, T., eds., Studies of Inner Piedmont geology with a focus on the Columbus Promontory: Carolina Geological Society Field Trip Guidebook, p. 55–66.

Gastaldo, R.A., Guthrie, G.M., and Steltenpohl, M.G., 1993, Mississippian fossils from southern Appalachian metamorphic rocks and their implications for late Paleozoic tectonic evolution: Science, v. 262, p. 732–734, doi:10.1126/science.262.5134.732.

Gates, A.E., Speer, J.A., and Pratt, T.L., 1988, The Alleghanian southern Appalachian Piedmont: A transpressional model: Tectonics, v. 7, p. 1307–1324, doi:10.1029/TC007i006p01307.

Goldstein, A., and Hepburn, J.C., 1999, Possible connections of the Norumbega fault system with faults in southeastern New England, *in* Ludman, A., and West, D.P., Jr., eds., Norumbega fault system in the northern Appalachians: Geological Society of America Special Paper 331, p. 73–83, doi:10.1130/0-8137-2331-0.73.

Guthrie, G.M., ed., 1995, The timing and tectonic mechanism of the Alleghanian orogeny, Alabama Piedmont: Alabama Geological Society 32nd Annual Field Trip Guidebook: Tuscaloosa, Alabama, Geological Survey of Alabama, 98 p.

Guthrie, G.M., and Raymond, D.E., 1992, Pre-Middle Jurassic rocks beneath the Alabama Gulf Coastal Plain: Geological Survey of Alabama Bulletin 150, 155 p.

Hadizadeh, J., Babaie, H.A., and Babaie, A., 1991, Development of interlaced mylonites, cataclasites and breccias: Example from the Towaliga fault, south-central Appalachians: Journal of Structural Geology, v. 13, p. 63–70, doi:10.1016/0191-8141(91)90101-N.

Hames, W.E., Tull, J.F., Barbeau, D.L., Jr., McDonald, W.M., and Steltenpohl, M.G., 2007, Laser $^{40}Ar/^{39}Ar$ ages of muscovite and evidence for Mississippian (Visean) deformation near the thrust front of the southwestern Blue Ridge province: Geological Society of America Abstracts with Programs, v. 39, no. 2, p. 78.

Hatcher, R.D., Jr., 1978, Tectonics of the western Piedmont and Blue Ridge, southern Appalachians: Review and speculation: American Journal of Science, v. 278, p. 276–304, doi:10.2475/ajs.278.3.276.

Hatcher, R.D., Jr., 1987, Tectonics of the southern and central Appalachian internides: Annual Review of Earth and Planetary Sciences, v. 15, p. 337–362, doi:10.1146/annurev.ea.15.050187.002005.

Hatcher, R.D., Jr., 1989, Tectonic synthesis of the U.S. Appalachians, *in* Hatcher, R.D., Jr., et al., eds., The Appalachian-Ouachita orogen in the United States: Boulder, Colorado, Geological Society of America, Geology of North America, v. F-2, p. 511–535.

Hatcher, R.D., Jr., 2002, The Alleghanian (Appalachian) orogeny, a product of zipper tectonics: Rotational transpressive continent-continent collision and closing of ancient oceans along irregular margins, *in* Martínez Catalán, J.R., et al., eds., Variscan-Appalachian dynamics: The building of the late Paleozoic basement: Geological Society of America Special Paper 364, p. 199–208, doi:10.1130/0-8137-2364-7.199.

Hatcher, R.D., Jr., 2004, Southeastern Tennessee–western North Carolina Blue Ridge scenery and tectonics: Ancient Laurentian margin and recycled billion-year old crust, 550 million year old ocean crust and mantle, and the 6,000+ ft spine of the eastern U.S.: Field trip guide: Oak Ridge, Tennessee, Oak Ridge Institute for Continued Learning, 40 p.

Hatcher, R.D., Jr., 2010, The Appalachian orogen: A brief summary, *in* Tollo, R.P., et al., eds., From Rodinia to Pangea: The lithotectonic record of the Appalachian region: Geological Society of America Memoir 206, p. 1–20, doi:10.1130/2010.1206(01).

Hatcher, R.D., Jr., and Merschat, A.J., 2006, The Appalachian Inner Piedmont: An exhumed strike-parallel, tectonically forced orogenic channel, *in* Law, R.D., et al., eds., Channel flow, ductile extrusion, and exhumation of lower–mid crust in continental collision zones: Geological Society of London Special Publication 268, p. 517–541, doi:10.1144/GSL.SP.2006.268.01.24.

Hatcher, R.D., Jr., Thomas, W.A., Geiser, P.A., Snoke, A.W., Mosher, S., and Wiltschko, D.V., 1989a, Alleghanian orogen, *in* Hatcher, R.D., Jr., et al., eds., The Appalachian-Ouachita orogen in the United States: Boulder, Colorado, Geological Society of America, Geology of North America, v. F-2, p. 233–318.

Hatcher, R.D., Jr., Osberg, P.H., Drake, A.A., Jr., Robinson, P., and Thomas, W.A., 1989b, Tectonic map of the U.S. Appalachians, *in* Hatcher, R.D., Jr., et al., eds., The Appalachian-Ouachita orogen in the United States: Boulder, Colorado, Geological Society of America, Geology of North America, v. F-2, Plate 1.

Hatcher, R.D., Jr., Bream, B.R., and Merschat, A.J., 2007a, Tectonic map of the Southern and Central Appalachians: USA. Plate 1, *in* Hatcher, R.D., Jr., et al., eds., The 4-D framework of continental crust: Geological Society of America Memoir 200, scale 1:2,000,000.

Hatcher, R.D., Jr., Lemiszki, P.J., and Whisner, J.B., 2007b, Character of the rigid boundaries and internal deformation of the southern Appalachian foreland fold-thrust belt, *in* Sears, J.W., et al., eds., Whence the mountains? Inquiries into the evolution of orogenic systems: A volume in honor of Raymond A. Price: Geological Society of America Special Paper 433, p. 243–276, doi:10.1130/2007.2433(12).

Hewitt, J.L., 1984, Geologic overview, coal and coalbed methane resources of the Black Warrior basin—Alabama and Mississippi, *in* Rightmire, C.T., et al., eds., Coalbed methane resources of the United States: American Association of Petroleum Geologists Studies in Geology Series 17, p. 73–104.

Hibbard, J.P., Stoddard, E.F., Secor, D.T., Jr., and Dennis, A.J., 2002, The Carolina Zone: Overview of Neoproterozoic to early Paleozoic peri-Gondwanan terranes along the eastern flank of the southern Appalachians: Earth-Science Reviews, v. 57, p. 299–339, doi:10.1016/S0012-8252(01)00079-4.

Hibbard, J.P., van Staal, C.R., Rankin, D.W., and Williams, H., 2006, Lithotectonic map of the Appalachian orogen, Canada–United States of America: Geological Survey of Canada Map 2096A, scale 1:1,500,000.

Higgins, M.W., Atkins, R.L., Crawford, T.J., Crawford, R.F., Brooks, R., and Cook, R.B., 1988, The structure, stratigraphy, tectonostratigraphy and evolution of the southernmost part of the Appalachian orogen: U.S. Geological Survey Professional Paper 1475, 173 p.

Hirth, G., and Tullis, J.A., 1992, Dislocation creep regimes in quartz aggregates: Journal of Structural Geology, v. 14, p. 145–159, doi:10.1016/0191-8141(92)90053-Y.

Hirth, G., and Tullis, J., 1994, The nature of the brittle to plastic transition in quartz aggregates: Journal of Geophysical Research, v. 99, p. 11,731–11,748, doi:10.1029/93JB02873.

Hodges, K.V., Parrish, R.R., Housh, T.B., Lux, D.R., Burchfiel, B.C., Royden, L.H., and Chen, Z., 1992, Simultaneous Miocene extension and shortening in the Himalayan orogeny: Science, v. 258, p. 1466–1470, doi:10.1126/science.258.5087.1466.

Hooper, R.J., and Hatcher, R.D., Jr., 1988, Pine Mountain terrane, a complex window in the Georgia and Alabama Piedmont: Evidence from the eastern termination: Geology, v. 16, p. 307–310, doi:10.1130/0091-7613(1988)016<0307:PMTACW>2.3.CO;2.

Hooper, R.J., Hatcher, R.D., Jr., Troyer, P.K., Dawson, R.J., and Redmon, C.G., 1997, The character of the Avalon terrane and its boundary with the Piedmont terrane in central Georgia, *in* Glover, L., III, and Gates, A.E., eds., Central and southern Appalachian sutures: Results of the EDGE Project and related studies: Geological Society of America Special Paper 314, p. 1–14, doi:10.1130/0-8137-2314-0.1.

Horton, J.W., Jr., Avery, A.D., Jr., and Rankin, D.W., 1989, Tectonostratigraphic terranes and their Paleozoic boundaries in the central and southern Appalachians, *in* Dallmeyer, R.D., ed., Terranes in the circum-Atlantic Paleozoic orogens: Geological Society of America Special Paper 230, p. 213–245, doi:10.1130/SPE230-p213.

Huebner, M.T., and Hatcher, R.D., Jr., 2011, Evidence for sinistral Mesozoic inversion of the dextral Alleghanian Towaliga fault, central Georgia, *in* Huebner, M.T., and Hatcher, R.D., Jr., eds., The geology of the Inner Piedmont at the northeast end of the Pine Mountain window: Georgia Geological Society Annual Field Trip Guidebook, v. 31, p. 55–72.

Huebner, M.T., Hatcher, R.D., Jr., and Davis, B.A., 2010, Extent, kinematics, and Mesozoic reactivation of the Alleghanian Towaliga fault, central Georgia Appalachians: Geological Society of America Abstracts with Programs, v. 42, no. 1, p. 128.

Ingram, S., Schwartz, J.J., and Johnson, K., 2011, U-Pb zircon and monzonite geochronology and Hf isotope geochemistry of Neoacadian and early Alleghanian plutonic rocks in the Alabama eastern Blue Ridge, southern Appalachian Mountains: Geological Society of America Abstracts with Programs, v. 43, no. 5, p. 88.

Keranen, K., and Klemperer, S.L., 2008, Discontinuous and diachronous evolution of the Main Ethiopian Rift: Implications for development of continental rifts: Earth and Planetary Science Letters, v. 265, p. 96–111, doi:10.1016/j.epsl.2007.09.038.

Klitgord, K.D., Hutchinson, D.R., and Schouten, H., 1988, U.S. Atlantic coastal margin: Structural and tectonic framework, *in* Sheridan, R.E., and Grow, J.A., eds., The Atlantic continental margin: U.S.: Boulder, Colorado, Geological Society of America, Geology of North America, v. I-2, p. 19–55.

Kohn, M.J., 2001, Timing of arc accretion in the southern Appalachians: Perspectives from the Laurentian margin: Geological Society of America Abstracts with Programs, v. 33, no. 6, p. A262.

Ludwig, K.R., 1989, Pb.Dat: A computer program for processing raw Pb-U-Th isotope data: U.S. Geological Survey Open-File Report 88, 557 p.

Maher, H.D., Jr., Dallmeyer, R.D., Secor, D.T., Jr., and Sacks, P.E., 1994, $^{40}Ar/^{39}Ar$ constraints on chronology of Augusta fault zone movement and late Alleghanian extension, southern Appalachian Piedmont, S.C. & Ga: American Journal of Science, v. 294, p. 428–448, doi:10.2475/ajs.294.4.428.

Massey, M.A., and Moecher, D.P., 2005, Deformation and metamorphic history of the Western Blue Ridge–Eastern Blue Ridge terrane boundary, southern Appalachian Orogen: Tectonics, v. 24, doi:10.1029/2004TC001643.

McBride, J.H., Hatcher, R.D., Jr., Stephenson, W.J., and Hooper, R.J., 2005, Integrating seismic reflection and geological data and interpretations across an internal basement massif: The southern Appalachian Pine Mountain window, USA: Geological Society of America Bulletin, v. 117, p. 669–686, doi:10.1130/B25313.1.

McClellan, E.A., Steltenpohl, M.G., Thomas, C., and Miller, C.F., 2005, Isotopic age constraints and metamorphic history of the Talladega belt: New evidence for timing of arc magmatism and terrane emplacement along the southern Laurentian margin, *in* Steltenpohl, M.G., ed., Southernmost Appalachian terranes, Alabama and Georgia: Geological Society of America Southeastern Section Field Trip Guidebook: Tuscaloosa, Geological Survey of Alabama, p. 19–50.

McClellan, E.A., Steltenpohl, M.G., Thomas, C., and Miller, C., 2007, Isotopic age constraints and metamorphic history of the Talladega belt: New evidence for timing of arc magmatism and terrane emplacement along the southern Laurentian margin: Journal of Geology, v. 115, p. 541–561, doi:10.1086/519777.

McConnell, K.I., and Costello, J.O., 1980, Guide to geology along a traverse through the Blue Ridge and Piedmont Provinces of north Georgia, *in* Frey, R.W., ed., Excursions in southeastern geology, Volume 1: Falls Church, Virginia, American Geological Institute, p. 241–258.

McDonald, W.M., Hames, W.E., Marzen, L.J., and Steltenpohl, M.G., 2007, A GIS database for $^{40}Ar/^{39}Ar$ data of the southwestern Blue Ridge province: Geological Society of America Abstracts with Programs, v. 39, no. 2, p. 81.

McDougall, I., and Harrison, T.M., 1999, Geochronology and thermochronology by the $^{40}Ar/^{39}Ar$ method (second edition): New York, Oxford University Press, 269 p.

McNulty, B.A., Farber, D.L., Wallace, G.S., Lopez, R., and Palacios, O., 1998, Role of plate kinematics and plate-slip-vector partitioning in continental magmatic arcs: Evidence from the Cordillera Blanca, Peru: Geology, v. 26, p. 827–830, doi:10.1130/0091-7613(1998)026<0827:ROPKAP>2.3.CO;2.

Mercier, J.L., Sebrier, M., Lavenu, A., Cabrera, L., Bellier, O., Dumont, J.F., and Machare, J., 1992, Changes in the tectonic regime above a subduction zone of Andean type: The Andes of Peru and Bolivia during the Pliocene-Pleistocene: Journal of Geophysical Research, v. 97, p. 11,945–11,982, doi:10.1029/90JB02473.

Merschat, A.J., Hatcher, R.H., Jr., and Davis, T.L., 2005, The northern Inner Piedmont, Southern Appalachians, USA: Kinematics of transpression and SW-directed mid-crustal flow: Journal of Structural Geology, v. 27, p. 1252–1281, doi:10.1016/j.jsg.2004.08.005.

Merschat, A.J., Hatcher, R.D., Jr., Stahr, D.W., III, Cyphers, S.R., and Eckert, J.O., 2007, Detailed geologic mapping in the Great Balsam and Cowee mountains, central and eastern Blue Ridge, western North Carolina: Geological Society of America Abstracts with Programs, v. 39, no. 2, p. 99.

Mies, J.W., 1991, Structural geology of the Hightower Embayment, southern Cleburne County, Alabama: Geological Survey of Alabama Circular 156, 61 p.

Moore, W.B., Tull, J.F., and Allison, D.T., 1987, Intrusive chronology, progressive deformation, and geochemistry of granitoid dikes and strain analysis of xenoliths, Northern Piedmont, Tallapoosa County, Alabama, *in* Drummond, M.S., and Green, N.L., eds., Granites of Alabama: Tuscaloosa, Geological Survey of Alabama, p. 33–56.

Muangnoicharoen, N., 1975, The geology and structure of a portion of the northern piedmont, east-central Alabama [M.S. thesis]: Tuscaloosa, University of Alabama, 72 p.

Neathery, T.L., and Reynolds, J.W., 1973, Stratigraphy and metamorphism of the Wedowee Group—A reconnaissance: American Journal of Science, v. 273, p. 723–741, doi:10.2475/ajs.273.8.723.

Neathery, T.L., and Reynolds, J.W., 1975, Geology of the Lineville East, Ofelia, Wadley North and Mellow Valley quadrangles, Alabama: Geological Survey of Alabama Bulletin 109, 120 p.

Nelson, K.D., Arnow, J.A., Giguere, M., and Schamel, S., 1987, Normal-fault boundary of an Appalachian basement massif? Results of COCORP profiling across the Pine Mountain belt in western Georgia: Geology, v. 15, p. 832–836, doi:10.1130/0091-7613(1987)15<832:NBOAAB>2.0.CO;2.

Osborne, W.E., Szabo, M.W., Neathery, T.L., and Copeland, C.W., Jr., compilers, 1988, Geologic map of Alabama, northeast sheet: Alabama Geological Survey Special Map 220, scale 1:250,000.

Passchier, C.W., and Trouw, R.A.J., 1996, Microtectonics: Berlin, Springer, 289 p.

Pindell, J., and Dewey, J.F., 1982, Permo-Triassic reconstruction of western Pangea and the evolution of the Gulf of Mexico/Caribbean region: Tectonics, v. 1, p. 179–211, doi:10.1029/TC001i002p00179.

Pindell, J.L., Kennan, L., and Barrett, S.F., 2000, Putting it all together again: American Association of Petroleum Geologists Explorer, October.

Ratajeski, K., Glazner, A.J., and Miller, B.V., 2001, Geology and geochemistry of mafic to felsic plutonic rocks in the Cretaceous intrusive suite of Yosemite Valley, California: Geological Society of America Bulletin, v. 113, p. 1486–1502, doi:10.1130/0016-7606(2001)113<1486:GAGOMT>2.0.CO;2.

Raymond, D.E., Osborne, W.E., Copeland, C.W., and Neathery, T.L., 1988, Alabama stratigraphy: Tuscaloosa, Geological Survey of Alabama, 97 p.

Roeder, D., Gilbert, O.E., and Witherspoon, W.D., 1978, Evolution and macroscopic structure of the Valley and Ridge thrust belt, Tennessee and Virginia: Studies in geology 2: Knoxville, University of Tennessee Department of Geological Sciences, 25 p.

Russell, G.S., 1978, U-Pb, Rb-Sr, and K-Ar isotopic studies bearing on the development of the southernmost Appalachian orogen, Alabama [Ph.D. thesis]: Tallahassee, Florida State University, 197 p.

Sacks, P.E., and Secor, D.T., Jr., 1990, Kinematics of late Paleozoic continental collision between Laurentia and Gondwana: Science, v. 250, no. 4988, p. 1702–1705, doi:10.1126/science.250.4988.1702.

Salvador, A., 1991, Origin and development of the Gulf of Mexico Basin, *in* Salvador, A., ed., The Gulf of Mexico Basin: Boulder, Colorado, Geological Society of America, Geology of North America, v. J, p. 389–444.

Scholz, C.H., 1988, The brittle-plastic transition and depth of seismic faulting: Geologische Rundschau, v. 77, p. 319–328, doi:10.1007/BF01848693.

Schwartz, D.P., 1988, Paleoseismicity and neotectonics of the Cordillera Blanca fault zone, northern Peruvian Andes: Journal of Geophysical Research, v. 93, no. B5, p. 4712–4730, doi:10.1029/JB093iB05p04712.

Schwartz, J.J., Johnson, K., and Ingram, S., 2011a, U-Pb zircon geochronology of Neoacadian and early Alleghenian plutonic rocks in the Alabama Eastern Blue Ridge, Southern Appalachian Mountains: Geological Society of America Abstracts with Programs, v. 43, no. 1, p. 62.

Schwartz, J.J., Johnson, K., Miranda, E.A., and Wooden, J.W., 2011b, The generation of high Sr/Y plutons following Late Jurassic arc-arc collision, Blue Mountains, NE Oregon: Lithos, v. 126, p. 22–41, doi:10.1016/j.lithos.2011.05.005.

Secor, D.T., Snoke, A.W., and Dallmeyer, R.D., 1986, Character of the Alleghanian orogeny in the southern Appalachians: Part III, Regional tectonic relations: Geological Society of America Bulletin, v. 97, p. 1345–1353, doi:10.1130/0016-7606(1986)97<1345:COTAOI>2.0.CO;2.

Selverstone, J., 2005, Are the Alps collapsing?: Annual Reviews of Earth and Planetary Science, v. 33, p. 113–132, doi:10.1146/annurev.earth.33.092203.122535.

Sibson, R.H., 1977, Fault rocks and fault mechanics: Geological Society of London Journal, v. 133, p. 191–213, doi:10.1144/gsjgs.133.3.0191.

Simpson, C., and Schmid, S., 1983, An evaluation of criteria to deduce the sense of movement in sheared rocks: Geological Society of America Bulletin, v. 94, p. 1281–1288, doi:10.1130/0016-7606(1983)94<1281:AEOCTD>2.0.CO;2.

Snoke, A.W., and Frost, B.R., 1990, Exhumation of high pressure politic schist, Lake Murray spillway, South Carolina: Evidence for crustal extension during Alleghanian strike-slip faulting: American Journal of Science, v. 290, p. 853–881, doi:10.2475/ajs.290.8.853.

Stacey, J.S., and Kramers, J.D., 1975, Approximation of terrestrial lead isotope evolution by a two-stage model: Earth and Planetary Science Letters, v. 26, p. 207–221.

Stahr, D.W., III, Hatcher, R.D., Jr., Miller, C.F., and Wooden, J.L., 2006, Alleghanian deformation in the Georgia and North Carolina eastern Blue Ridge: Insights from pluton ages and fabrics: Geological Society of America Abstracts with Programs, v. 38, no. 3, p. 20.

Steiner, M.B., 2005, Pangean reconstruction of the Yucatan Block: Its Permian, Triassic, and Jurassic geologic and tectonic history, *in* Anderson, T.H., et al., eds., The Mojave-Sonora megashear hypothesis: Development, assessment, and alternatives: Geological Society of America Special Paper 393, p. 457–480, doi:10.1130/0-8137-2393-0.457.

Steltenpohl, M.G., 1988, Kinematics of the Towaliga, Bartletts Ferry, and Goat Rock fault zones, Alabama: The late Paleozoic dextral shear system in the southernmost Appalachians: Geology, v. 16, p. 852–855, doi:10.1130/0091-7613(1988)016<0852:KOTTBF>2.3.CO;2.

Steltenpohl, M.G., 1992, The Pine Mountain window of Alabama: Basement-cover evolution in the southernmost exposed Appalachians, *in* Bartholomew, M.J., et al., eds., Basement tectonics 8: Characterization of ancient and Mesozoic continental margins: Proceedings of the 8th International Conference on Basement Tectonics, Butte, Montana, 1988: Dordrecht, Netherlands, Kluwer Academic Publishers, p. 491–501.

Steltenpohl, M.G., ed., 2005, New perspectives on southernmost Appalachian terranes, Alabama and Georgia: Alabama Geological Society 42nd Annual Field Trip Guidebook, 212 p.

Steltenpohl, M.G., and Kunk, M.J., 1993, $^{40}Ar/^{39}Ar$ thermochronology and Alleghanian development of the southernmost Appalachian Piedmont, Alabama and southwest Georgia: Geological Society of America Bulletin, v. 105, p. 819–833, doi:10.1130/0016-7606(1993)105<0819:AATAAD>2.3.CO;2.

Steltenpohl, M.G., and Moore, W.B., 1988, Metamorphism in Alabama: Geological Survey of Alabama Circular 138, 29 p.

Steltenpohl, M.G., Guthrie, G.M., and Cook, R.B., 1990a, Geology of the Brevard zone at Jacksons Gap, Alabama, *in* Steltenpohl, M.G., et al., eds., Geology of the southern Inner Piedmont, Alabama and southwest Georgia: Geological Society of America Southeastern Section Field Trip Guidebook: Tuscaloosa, Geological Survey of Alabama, p. 101–110.

Steltenpohl, M.G., Neilson, M.J., and Kish, S.A., eds., 1990b, Geology of the southern Inner Piedmont, Alabama and southwest Georgia: Geological Society of America Southeastern Section Field Trip Guidebook: Tuscaloosa, Geological Survey of Alabama, 138 p.

Steltenpohl, M.G., Goldberg, S.A., Hanley, T.B., and Kunk, M.J., 1992, Evidence for Alleghanian development of the Goat Rock fault zone, Alabama and southwest Georgia: Temporal compatibility with the master décollement: Geology, v. 20, p. 845–848, doi:10.1130/0091-7613(1992)020<0845:ADOTGR>2.3.CO;2.

Steltenpohl, M.G., Gastaldo, R.A., Yokel, L., Heatherington, A., and Mueller, P., 1996, New U-Pb and $^{40}Ar/^{39}Ar$ dates from the Alabama Piedmont and plateau: Geological Society of America Abstracts with Programs, v. 28, no. 2, p. 45.

Steltenpohl, M.G., Miller, B.V., and Sterling, W., 2003, Tectonic implications of a 369 Ma U-Pb zircon date on granitic dikes cutting right-slip shears associated with the Alexander City fault zone, Alabama: Geological Society of America Abstracts with Programs, v. 35, no. 2, p. 7.

Steltenpohl, M.G., Hames, W.E., and Andresen, A., 2004a, The Silurian to Permian history of a metamorphic core complex in Lofoten, northern Scandinavian Caledonides: Tectonics, v. 23, TC1002, p. 1–23, doi:10.1029/2003TC001522.

Steltenpohl, M.G., Heatherington, A., Mueller, P., and Wooden, J.L., 2004b, Pre-Appalachian tectonic evolution of the Pine Mountain window in the southernmost Appalachians, Alabama and Georgia, *in* Tollo, R.P., et al., eds., Proterozoic tectonic evolution of the Grenville orogen in North America: Geological Society of America Memoir 197, p. 633–646, doi:10.1130/0-8137-1197-5.633.

Steltenpohl, M.G., Mueller, P., Heatherington, A., Hanley, T.B., and Wooden, J.L., 2008, Gondwanan/Peri-Gondwanan origin for the Uchee terrane, Alabama and Georgia: Carolina zone or Suwannee terrane(?) and its suture with Grenvillian basement of the Pine Mountain window: Geosphere, v. 4, p. 131–144, doi:10.1130/GES00079.1.

Steltenpohl, M.G., Hatcher, R.D., Jr., Mueller, P.A., Heatherington, A.L., and Wooden, J.L., 2010, Geologic history of the Pine Mountain window, Alabama and Georgia: Insights from a new geologic map and U-Pb isotopic dates, *in* Tollo, R.P., et al., eds., From Rodinia to Pangea: The lithotectonic record of the Appalachian region: Geological Society of America Memoir 206, p. 837–858, doi:10.1130/2010.1206(32).

Steltenpohl, M.G., Moecher, D.P., Andersen, A., Ball, J.B., Mager, S.M., and Hames, W.E., 2011, The Eidsfjord shear zone, Lofoten-Vesterålen, north Norway: An Early Devonian, paleoseismogenic low-angle normal fault: Journal of Structural Geology, v. 33, p. 1023–1043, doi:10.1016/j.jsg.2011.01.017.

Sterling, J.W., 2006, Geology of the southernmost exposures of the Brevard zone in the Red Hill Quadrangle, Alabama [M.S. thesis]: Auburn, Alabama, Auburn University, 118 p.

Sterling, J.W., Steltenpohl, M.G., and Cook, R.B., 2005, Geology of the southern exposures of the Brevard zone in the Red Hill Quadrangle near Martin Dam, Alabama, *in* Steltenpohl, M.G., ed., Southernmost Appalachian terranes, Alabama and Georgia: Geological Society of America Southeastern Section Field Trip Guidebook: Tuscaloosa, Geological Survey of Alabama, p. 70–97.

Stewart, K.G., and Miller, B.V., 2001, The tectonic implications of 460 Ma eclogite along the Taconian suture in the eastern Blue Ridge of North Carolina: Geological Society of America Abstracts with Programs, v. 33, no. 6, p. A-65.

Stow, S.H., and Tull, J.F., 1979, Geologic mapping of the Turkey Heaven Mountain region, Cleburne and Randolf counties, Alabama: Alabama Geological Survey Open-File Report, 30 p.

Stowell, H.H., Lesher, C.M., Gren, N.L., and Sha, P., 1996, Metamorphism and gold mineralization in the Blue Ridge southernmost Appalachians: Economic Geology and the Bulletin of the Society of Economic Geologists, v. 91, p. 1115–1144, doi:10.2113/gsecongeo.91.6.1115.

Thomas, W.A., 1991, The Appalachian–Ouachita rifted margin of southeastern North America: Geological Society of America Bulletin, v. 103, p. 415–431, doi:10.1130/0016-7606(1991)103<0415:TAORMO>2.3.CO;2.

Thomas, W.A., 2006, Tectonic inheritance at a continental margin: GSA Today, v. 16, no. 2, p. 4–11, doi:10.1130/1052-5173(2006)016[4:TIAACM]2.0.CO;2.

Thomas, W.A., and Neathery, T.L., 1980, Tectonic framework of the Appalachian orogen in Alabama, *in* Frey, R.W., ed., Excursions in southeastern geology, Volume 2: Falls Church, Virginia, American Geological Institute, p. 465–526.

Thomas, W.A., and Steltenpohl, M.G., 2010, Truncation of the Iapetan rifted margin on the Alabama Promontory by the Suwannee-Wiggins suture: Geological Society of America Abstracts with Programs, v. 42, no. 1, p. 147.

Thomas, W.A., Neathery, T.N., and Ferrill, B.A., 1989, Cross-section A-A′, *in* Hatcher, R.D., Jr., et al., eds., The Appalachian-Ouachita orogen in the United States: Boulder, Colorado, Geological Society of America, Geology of North America, v. F-2.

Trupe, C.H., Stewart, K.G., Adams, M.G., Waters, C.L., Miller, B.V., and Hewitt, L.K., 2003, The Burnsville fault: Evidence for the timing and kinematics of southern Appalachian Acadian dextral transform tectonics: Geological Society of America Bulletin, v. 115, p. 1365–1376, doi:10.1130/B25256.1.

Tull, J.F., 1978, Structural development of the Alabama Piedmont Northwest of the Brevard Zone: American Journal of Science, v. 278, p. 442–460, doi:10.2475/ajs.278.4.442.

Tull, J.F., 1980, Overview of the sequence and timing of deformational events in the Southern Appalachians; evidence from the crystalline rocks, North Carolina to Alabama, *in* Wones, D.R., ed., The Caledonides in the USA: Virginia Polytechnic Institute Department of Geological Sciences Memoir 2, p. 167–177.

Tull, J.F., 1982, Stratigraphic framework of the Talladega slate terrane, Alabama Appalachians, *in* Bearce, D.N., et al., eds., Tectonic studies in the Talladega and Carolina slate belts, southern Appalachian orogen: Geological Society of America Special Paper 191, scale 1:1,370,000.

Tull, J.F., 1984, Polyphase late Paleozoic deformation in the southeastern foreland and northwestern Piedmont of the Alabama Appalachians: Journal of Structural Geology, v. 6, p. 223–234, doi:10.1016/0191-8141(84)90047-6.

Tull, J.F., 1995, Hollins Line transpressional duplex: Eastern-Western Blue Ridge terrain boundary: Geological Society of America Abstracts with Programs, v. 27, no. 2, p. 93.

Tull, J.F., 2011, Significance of late extensional faults in the southwestern Appalachian Blue Ridge: Geological Society of America Abstracts with Programs, v. 43, no. 2, p. 15.

Tull, J.F., and Holm, C.S., 2005, Structural evolution of a major Appalachian salient-recess junction: Consequences of oblique collisional convergence across a continental margin transform fault: Geological Society of America Bulletin, v. 117, p. 482–499, doi:10.1130/B25578.1.

Tull, J.F., Moore, W.B., Drummond, M.S., and Allison, D.T., 1985, Contrasting fault systems in the crystalline Appalachians of Alabama: Geological Society of America Abstracts with Programs, v. 17, p. 139.

Tull, J.F., Harris, A.G., Repetski, J.E., McKinney, F.K., Garrett, C.B., and Bearce, D.N., 1988, New paleontologic evidence constraining the age and paleotectonic setting of the Talladega slate belt, southern Appalachians: Geological Society of America Bulletin, v. 100, p. 1291–1299, doi:10.1130/0016-7606(1988)100<1291:NPECTA>2.3.CO;2.

Tull, J.F., Kish, S.A., Groszos, M.S., and Campbell, S.K., 1998a, Laurentian magmatism of the southern Appalachian Blue Ridge: Post-Iapetan rifting: Geological Society of America Bulletin, v. 110, p. 1281–1303, doi:10.1130/0016-7606(1998)110<1281:LMOTSA>2.3.CO;2.

Tull, J.F., Ragland, P.C., and Durham, R.B., 1998b, Geologic, geochemical, and tectonic setting of felsic metavolcanic rocks along the Alabama recess, southern Appalachian Blue Ridge: Southeastern Geology, v. 38, p. 39–64.

Tull, J.F., Barineau, C.I., Mueller, P.A., and Wooden, J.L., 2007, Volcanic arc emplacement onto the southernmost Appalachian Laurentian shelf: Characteristics and constraints: Geological Society of America Bulletin, v. 119, p. 261–274, doi:10.1130/B25998.1.

Tull, J.F., Mueller, P.A., Barineau, C.I., and Wooden, J.L., 2009, Age and tectonic implications of the Elkahatchee Quartz Diorite, Eastern Blue Ridge Province, southern Appalachians, USA: Geological Society of America Abstracts with Programs, v. 41, no. 7, p. 288.

Tullis, J.A., 1983, Deformation of feldspars, *in* Ribbe, P.H., ed., Feldspar mineralogy: Mineralogical Society of America Short Course Notes, v. 2, p. 297–323.

Tullis, J., 2002, Deformation of granitic rocks: Experimental studies and natural examples, *in* Karato, S.-I., and Wenk, H.-R., eds., Plastic deformation of minerals and rocks: Mineralogical Society of America Reviews in Mineralogy and Geochemistry Volume 51, p. 97–120.

Tullis, J., and Yund, R.A., 1992, The brittle-ductile transition in feldspar aggregates: An experimental study, *in* Evans, B., and Wong, T.F., eds., Fault mechanics and transport properties of rocks: New York, Academic Press, p. 89–118.

Vauchez, A., 1987, Brevard fault zone, southern Appalachians: A medium-angle, dextral, Alleghanian shear zone: Geology, v. 15, p. 669–672, doi:10.1130/0091-7613(1987)15<669:BFZSAA>2.0.CO;2.

Wampler, J.M., Neathery, T.L., and Bentley, R.D., 1970, Age relations in the Alabama Piedmont, *in* Bentley, R.D., and Neathery, T.L., eds., Geology of the Brevard fault zone and related rocks of the Inner Piedmont of Alabama: Alabama Geological Society 8th Annual Field Trip Guidebook, p. 81–90.

Wernicke, B., 1985, Uniform-sense simple shear of the continental lithosphere: Canadian Journal of Earth Sciences, v. 22, p. 108–125, doi:10.1139/e85-009.

West, T.E., Jr., Secor, D.T., Jr., Pray, J.R., Boland, I.B., and Maher, H.D., Jr., 1995, New field evidence for an exposure of the Appalachian décollement at the east end of the Pine Mountain terrane, Georgia: Geology, v. 23, p. 621–624, doi:10.1130/0091-7613(1995)023<0621:NFEFAE>2.3.CO;2.

Wielchowsky, C.C., 1983, The geology of the Brevard zone and adjacent terranes in Alabama [Ph.D. thesis]: Houston, Texas, Rice University, 237 p.

Wilson, G.V., and Zietz, I., 2002, Aeromagnetic map of Alabama: Geological Survey of Alabama State Oil and Gas Board Special Map 8B, scale 1:500,000.

Woodward, H.P., 1957, Chronology of Appalachian folding: American Association of Petroleum Geologists Bulletin, v. 41, p. 2312–2327.